**IRAQI BULLETIN OF GEOLOGY AND MINING (IBGM)**
**IRAQ GEOLOGICAL SURVEY (GEOSURV-IRAQ)**

***Vol.20, No.1, 2024*** ***p 103 – 126***

# GEOCHEMISTRY OF BROWN DETRITAL LIMESTONE BEDS WITHIN SARMORD FORMATION, SULAIMANI, KURDISTAN REGION, IRAQ: IMPLICATION FOR DEPOSITIONAL ENVIRONMENT, PROVENANCE AND TECTONIC SETTING

**Sardar M. Ridha[1*] and Sehad A. Eminki[1]**

[1] Dept. of Geology, College of Science-Sulaimani University
[*]Correspondence e-mail: sardar.ridha@univsul.edu.iq, Sardar M. Ridha
e-mail: sehad.asaad.m@gmail.com

*Type of the Paper: Article*
*Received: 14/ 01/ 2023*
*Accepted: 09/ 03/ 2023*

**Keywords:** Sarmord Formation; Detrital limestone; Tectonic setting; Depositional environment; Provenance.

## ABSTRACT

Fifteen samples of brown detrital limestone beds within the Sarmord Formation from the Imbricated Zone (Qaiwan and Barzinjah sections) and High Folded Zone (Zewe section), Kurdistan region, NE-Iraq were analyzed. The analysis includes the major oxides, trace elements, and rare earth elements (REEs) to find out their provenance, tectonic setting, and depositional environment. These beds are mainly composed of detrital limestone in which calcite and traces of quartz are confirmed by XRD and the microscopic study. $Al_2O_3/TiO_2$, La/Sc, La/Co, Th/Sc, Cr/Th and Th/Cr ratios and {($TiO_2$ + $V_2O_3$) - (MgO/ (MgO + $Al_2O_3$)}, ($TiO_2$ - Ni), (La/Th - Hf), (La/Sc - Co/Th) diagrams reveal sourcing from the mixed carbonate platform and felsic rocks. The ratios of major, trace, and REE with PAAS values fall within the range of felsic rocks, which agree with Cretaceous western Iraq (present Western Desert) as a source of these beds. The (Rb – Sr – Ba) ternary diagram and (Sr/Ba-Sr/Rb) diagram display the distribution of the samples between the continental margin and inland field. Tectonically, these detrital limestones are transported from the erosion of the interior of the Arabian platform into deep marine and interbedded with the green marl. The V/Cr, U/Th, Ni/Co, and Sr/Ca ratios and diagram of $Al_2O_3$-V indicate deposition under shallow marine oxic to the dysoxic environment and transported to the deep marine. The paleoclimate index C-value, Sr/Cu ratio, and $SiO_2$ - ($Al_2O_3$ + $K_2O$ + $Na_2O$) diagram indicates hot arid conditions. Paleosalinity ratios Rb/K and Sr/Ba imply brackish to marine water conditions.

## جيوكيميائية الحجرالجيري البني داخل تكوين سارمورد، السليمانية، إقليم كردستان، شمال شرق العراق: لمعرفة منشأها وتكوينها التكتوني وبيئة ترسيبها

**سردارمحمد رضا و سيهاد اسعد امينكي**

**المستخلص**

تم تحليل خمسة عشر عينة من طبقات الحجرالجيري البني داخل تكوين سارمورد من المنطقة المتراكبة (مقاطع قايوان وبرزنجة) والمنطقة ذات الطيات العالية (في مقطع زيوي)، إقليم كردستان ، شمال شرق العراق بحثًا عن الأكاسيد الرئيسية والعناصر النزرة والعناصر الأرضية النادرة لمعرفة منشأها وتكوينها التكتوني وبيئة ترسيبها.

تتكون هذه الطبقات بشكل أساسي من الحجر الجيري الفتاتي والذي تم تأكيد وجود الكالسيت وآثار الكوارتز بواسطة حيود الأشعة السينية (XRD) والدراسة المجهرية. نسب $Al_2O_3/TiO_2$ و La/Sc و La/Co و Th/Sc و Cr/Th و Th/Cr و {$(TiO_2 + V_2O_3)$ - MgO/ $(MgO + Al_2O_3)$}، ($TiO_2$-Ni)، (La/Th - Hf) (La/Sc - Co/Th) والرسوم البيانية تشير الى أصلها المختلط من المنصات الكاربونية والصخورالكلسية. تندرج نسب العناصر الرئيسية والنزرة والنادرة مع قيم post-Archaean Australian shale (PAAS) ضمن نطاق الصخورالكلسية التي تتوافق مع العصر الطباشيري لغرب العراق المتمثل بالصحراء الغربية الحالية كمصدر لهذه الطبقات. يعرض الرسم التخطيطي الثلاثي (Rb - Sr - Ba) والرسم التخطيطي (Sr/Ba - Sr/Rb) توزيع العينات بين الحافة القارية والحقل الداخلي. تكتونياً هذه الأحجار الجيرية الفتاتية نقلت بعد التعرية من الجزء الداخلي للمنصة العربية إلى أعماق البحار وتداخلت مع المارل الأخضر. تشير نسب V/Cr و U/Th و Ni/Co و Sr/Ca ومخطط $Al_2O_3$-V إلى ترسيب ضحل تحت السطح في بيئة مؤكسدة إلى بيئة قليلة الاوكسجين ثم نقلت إلى أعماق البحر. يشير مؤشر المناخ القديم ومخططات Sr/Cu و $SiO_2$ - $(Al_2O_3 + K_2O + Na_2O)$ إلى ظروف جافة ساخنة ونسب الملوحة القديمة Rb/K و Sr/Ba تشير إلى ظروف المياه البحرية شديدة الملوحة.

## 1. INTRODUCTION

Geochemical study of major and trace elements can reveal information about the nature of the sediment, sedimentary rock origin, and depositional conditions (Nesbitt & Young, 1982; Taylor & McLennan, 1985). Sedimentary rock geochemical characteristics are directly tied to the tectonic setting of sedimentary basins (Bhatia & Crook, 1986). The distinction between individual units of clastic and carbonate layers was commonly done using the bulk chemical composition of sedimentary rocks (Bjørlykke, 1974). Soluble elements within carbonate, such as Vr, Mg, Cr, Ni, Cu, Na, Zn, P, Sr, U, and Mo can be used to represent the chemical composition of paleo seawaters (Tribovillard et al., 2006).

The Sarmord Formation (Valanginian-Aptian) was first defined by Bellen et al. (1959) in the Surdash anticline, Sulaimani government, Kurdistan region, Iraq. The formation's type section is 455 meters of uniform brown and blue marl with layers of argillaceous limestones (Bellen et al., 1959). The Sarmord Formation was fragmented by (Chatton & Hart, 1960) into three parts, lower, middle, and upper. Buday (1980) merged the lowest two sections to form the Lower Sarmord Formation, which is considered to be Berriasian-Aptian in age.

Previous works within the Sarmord Formation have mainly focused on stratigraphy, sedimentology, depositional environment, reservoir characteristics, and source rock potential (Fatah et al., 2023). According to Jassim & Goff (2006) from the outer shelf to the deep inner shelf environment is where the Sarmord Formation was formed. Al-Samarraie (2012) suggested that the Sarmord Formation might belong to the deep shelf margin of normal salinity while Ahmed et al. (2015) believed that the Sarmord Formation deposited in the outer shelf environment.

The current study examines the geochemistry of the brown detrital limestone beds of the Sarmord Formation in the Qaiwan, Barzinjah, and Zewe sections (Figures 1 and 2). The following paper aims to determine the tectonic setting, provenance, climate, salinity, and redox conditions for the brown detrital limestone beds of the Sarmord Formation.

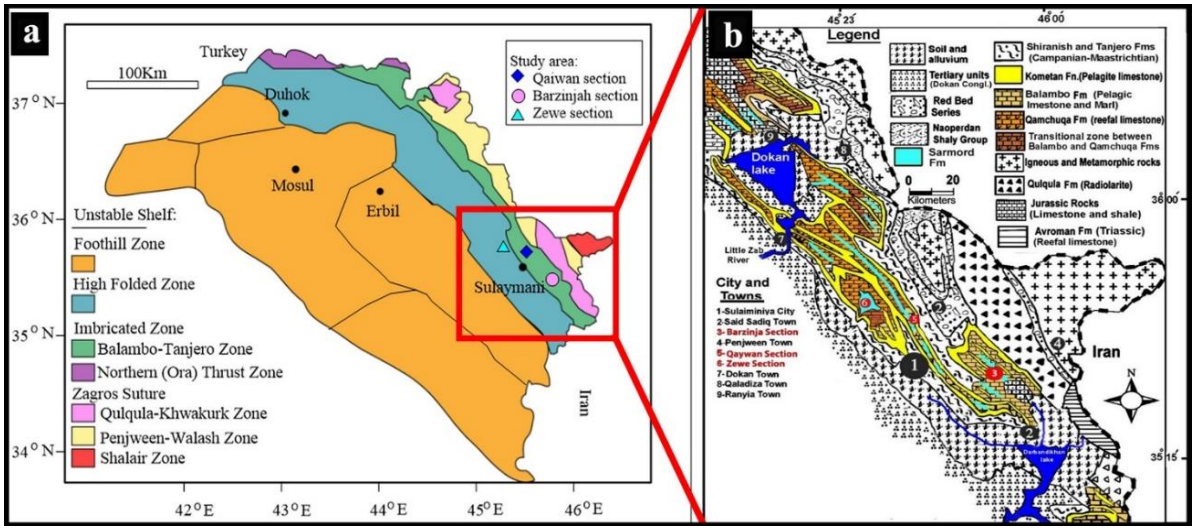


Figure 1: **a)** Tectonic subdivision of the Unstable Shelf of Iraq shown on the location map of Iraq (modified from Buday, T., and Jassim (1984); **b)** geological map of the study area (after Karim et al., 2021).


Figure 2: Field photos of **a)** Qaiwan section (intercalation of 7 brown beds of limestone with grey marl and marly limestone; **b)** Zewe section (only two thin beds of brown limestone); and **c)** Barzinjah section (intercalation 6 thin beds of brown limestone with grey marl and marly limestone).

## 2. GEOLOGICAL SETTING

The brown detrital limestones within the Sarmord Formation are studied throughout three sections: Qaiwan, Barzinjah, and Zewe. The first section is located 20 Km to the north of Sulaimani city, near the Little Qaiwan village at Latitude 35°42'32.53"N and longitude 45°25'18.30"E. This section is located in a small fold, which is a part of the major Azmir-Goizha anticline. It is a part of the Imbricated Zone of the Zagros Collisional Belt in the Iraqi tectonic subdivision of Jassim & Goff (2006) (Figure 1). Most outcrops of this formation are clear inside the core. The second section, which is located in the Imbricated zone is 1 Km from the South of the Barzinjah district at Latitude 35°32'34.25"N and longitude 45°41'44.62"E (Figure 1). The third section is located about 2 Km to the north of the Zewe district at Latitude 35°45'36.45"N and longitude 45°14'36.09"E in the High Folded Zone (Figure 1).

The Formation consists entirely of an alternation of marl, marly limestone, and detrital limestone (Figure 3). The Sarmord Formation has conformable contact with the Chia Gara and Balambo formations at the bottom and top, respectively in the Qaiwan (Figure 3a) and Barzinjah sections (Figure 3b). It overlaps the Chia Gara Formation and underlies the Qamchuqa Formation in the Zewe section (Figure 3c). It is clear from the study that thin sections look like detrital limestone with some diagenesis (Figure 4). The lower contacts of the beds are sharp and erosional indicating sudden deposition and high energy condition.

## 3. METHODS AND MATERIALS

Fifteen samples were collected along these three sections from the exposed outcrops of the formation, seven samples from Qaiwan, six samples from Barzinjah, and two samples from the Zewe section. Thin sections were made for fifteen rock samples at the University of Sulaimani/ Department of Geology for microscopic studies for petrographic study. Two bulk carbonate samples were analyzed using the X-ray diffraction technique (PANanalytical, Goniometer PW3050/60) in Sulaimani University/ Department of Geology to determine the mineral content.

Fine crushing of 15 samples to 70% passing 2 mm, then pulverize samples up to 250 g to 85% passing 75 microns. Major oxides of these samples of Sarmord Formation with (LOI) and some trace elements (Mo, Cu, Ni, Co, Zn, and SC) after fused bead and acid digestion were analyzed by using the inductively coupled plasma atomic emission spectrometry (ICP-AES). Most of the trace elements (Ba, Cr, Zr, U, Nb, V, Rb, Sr, Th, Y, and Hf) and rare earth elements (REEs) were analyzed after four acid digestion by using inductively coupled plasma-mass spectrometry (ICP-MS) in Canada at the ALS international laboratory. Chemical analysis has precisions of up to (0.01 to 3) % for major elements and (0.01 to 10) ppm for trace and REEs.

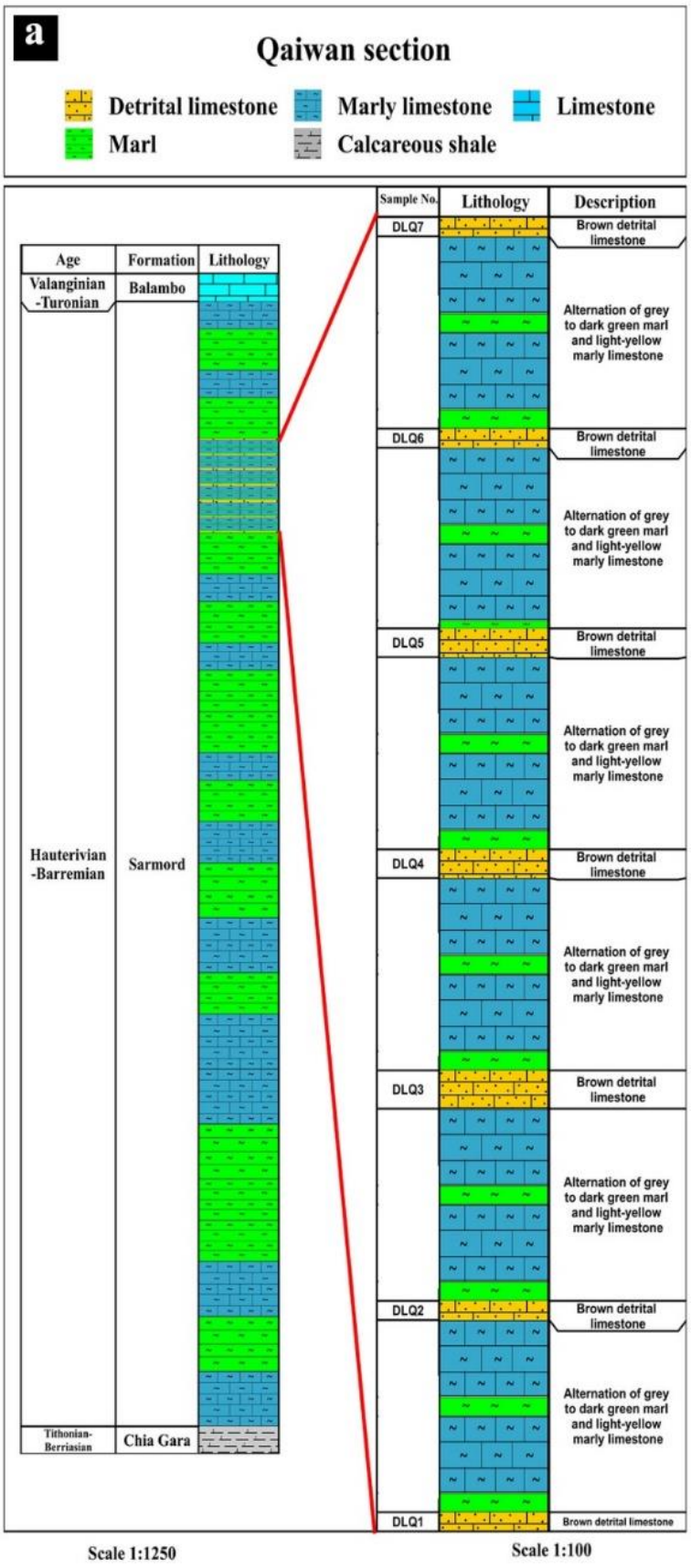


Figure 3: Columnar sections for Sarmord Formation in: (a) Qaiwan; (b) Barzinjah; (c) Zewe section.

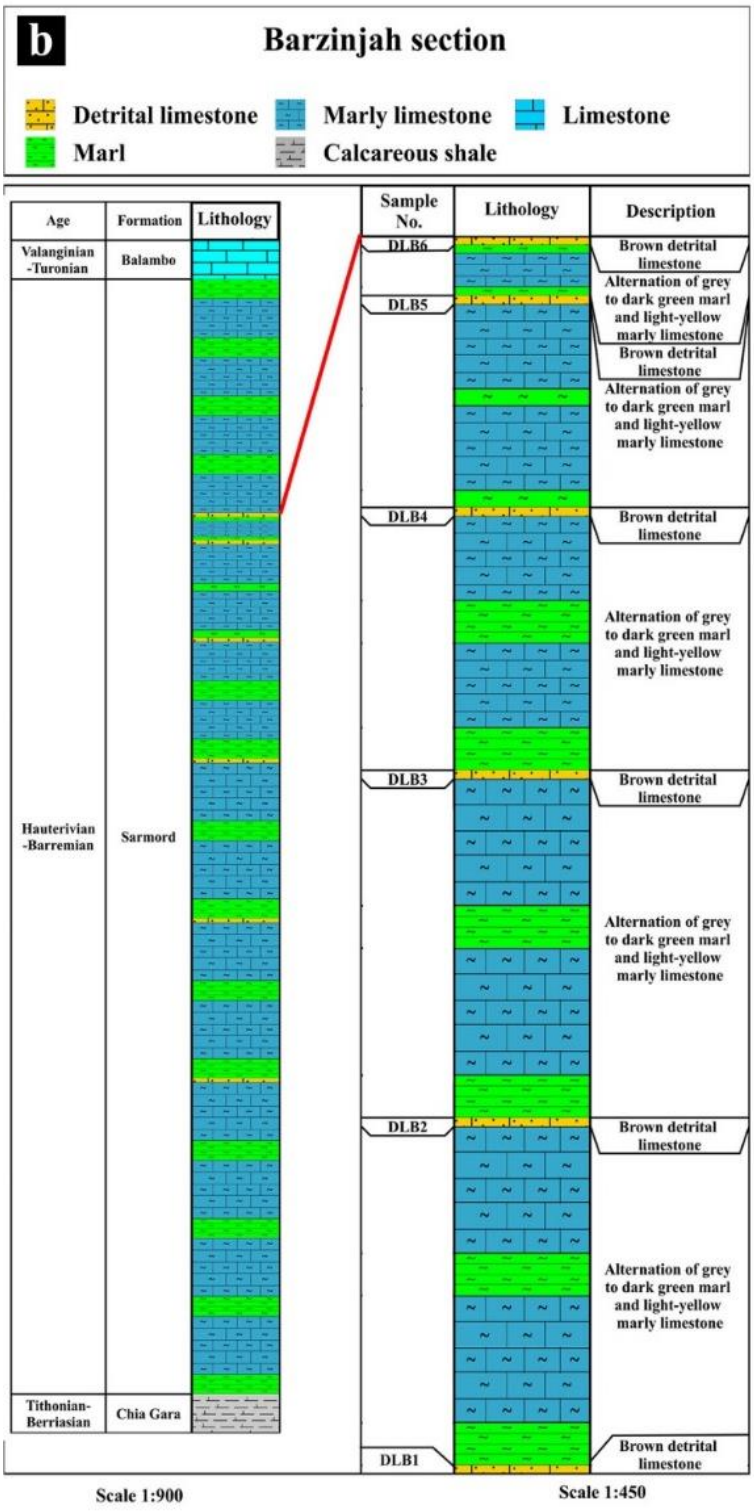


Figure 3: Continued.

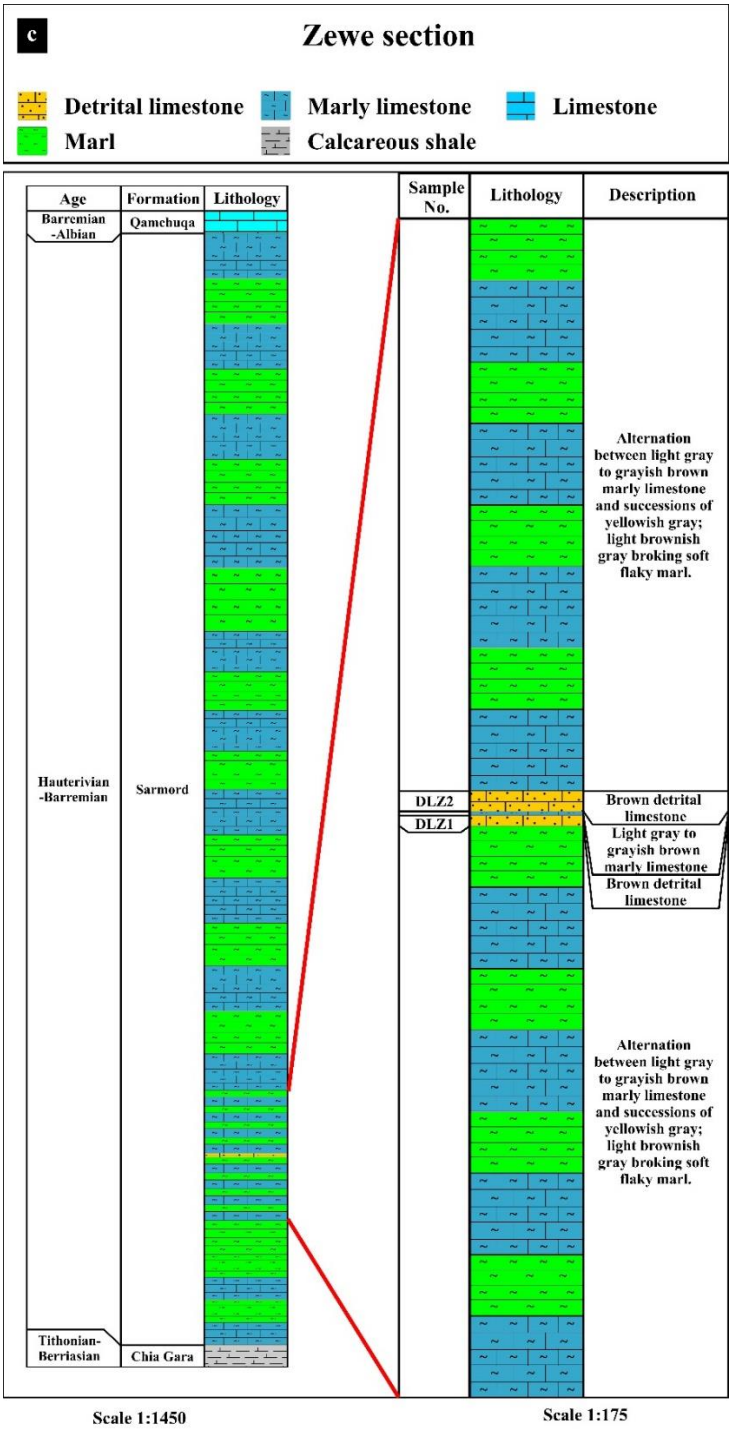


Figure 3: Continued.

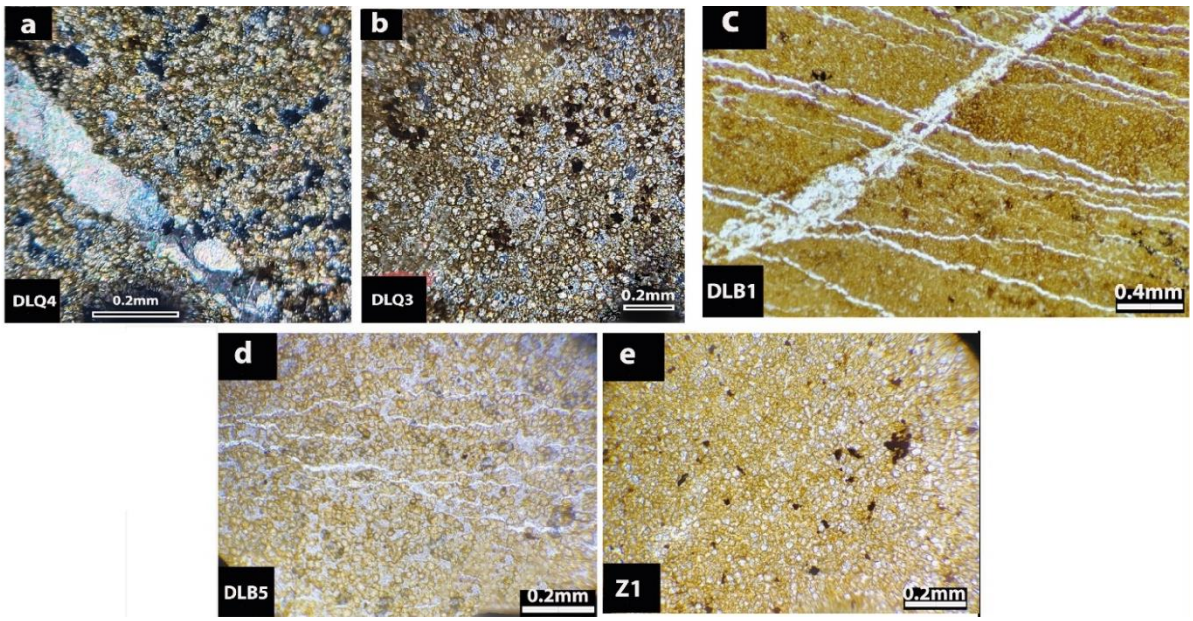


Figure 4: Photomicrographs under the polarized microscope of brown detrital limestone beds (partially recrystallized with dedolomitization) in Sarmord Formation, **(a** and **b)** represent samples DLQ4 and DLQ3 of Qaywan section contain a vein (filled by calcite) and iron oxide. XP light; **(c** and **d)** represent samples DLB1 and DLB5 of the Barzinja section showing fracturing due to unloading under stereoscope microscope; and **e)** Sample DLZ1 of Zewe section. It is observable that the brown layers, in all sections, are similar in petrographic properties.

## 4. RESULTS

The brown beds of the Sarmord Formation are characterized by thin-bedded streaks of limestone detrital, which is due to the high content of around 6 to 7% $Fe_2O_3$, fine crystalline calcareous ferruginous cemented. The iron comes from the source area, it is well known that source areas contain high iron content which has impacted on old sediments derived from them. It is fine crystalline, partly coarse to fine-grained, medium-hard, highly fractured in some places, and partly filled by calcite. Generally, these brown limestones in all sections are composed of detrital Limestone (Figure 4). Pellet and oolite are not present. All the beds have erosional sharp lower contact, which indicates possible calciturbidite.

From the XRD mineralogical point of view, these beds of limestones contain mainly calcite at $2\theta = 29.40°$ and traces of quartz at $2\theta = 26.6°$ (Figure 5). All samples were checked by calcimetry, XRD, and chemical analysis (ICP) showed that the beds are limestone, not dolomite.

### 4.1. Major oxides

The major components of 15 bulk samples were analyzed. Table 1 shows the brown beds are major oxide concentrations and loss on ignition (LOI) in (wt.%). Calcium oxide (CaO) % ranges between 33.8 to 39.9, which is the most abundant oxide in the examined rocks (average 36.41%) followed by little $SiO_2$ (9.66 to 15.55) % (average 14%) and $Fe_2O_3$ (6.24 to 7.65) % (average 7.08%).

In Barzinja section: CaO (38.5 to 46.8) % (average 40.57%), SiO2 (9.22 to 15.55) % (average 14%), Fe2O3 (2.57 to 6.11) % (average 4.56%). In the Zewe section: CaO (37.7 to 39.1) % (average 38.4%), SiO2 (9.97 to 11.25) % (average 10.61%), Fe2O3 (5.87 to 6.51) %

(average 6.19%). Low content of MgO is observed in all studied samples (average 1.9%, 0.68%, and 2.23%) in Qaiwan, Barzinjah, and Zewe sections, respectively. The average contents of $Na_2O$, $K_2O$, $Cr_2O_3$, $TiO_2$, MnO, $P_2O_5$, SrO, and BaO are very low (< 0.5 %) in all sections. Calcium oxide (CaO) shows a strong negative relation with $Al_2O_3$, $TiO_2$, $K_2O$, $Fe_2O_3$, $Cr_2O_3$, MgO, MnO and positive with LOI. It records a weak negative correlation with $SiO_2$, and weak positive with SrO. Significant positive relations of $Fe_2O_3$ were observed with $Al_2O_3$, MgO, $K_2O$, $TiO_2$, MnO, and $Cr_2O_3$ and negative with SrO and LOI (Table 2).

A spider graph is used to display normalized oxide patterns for the brown detrital limestone of the Sarmord Formation (Taylor & McLennan, 1985). Post Archian Australian Shale (PAAS) normalized oxide readings. (Figure 6). The average concentration of most oxides is less than the average values of the PAAS except Cao which has a greater concentration value.

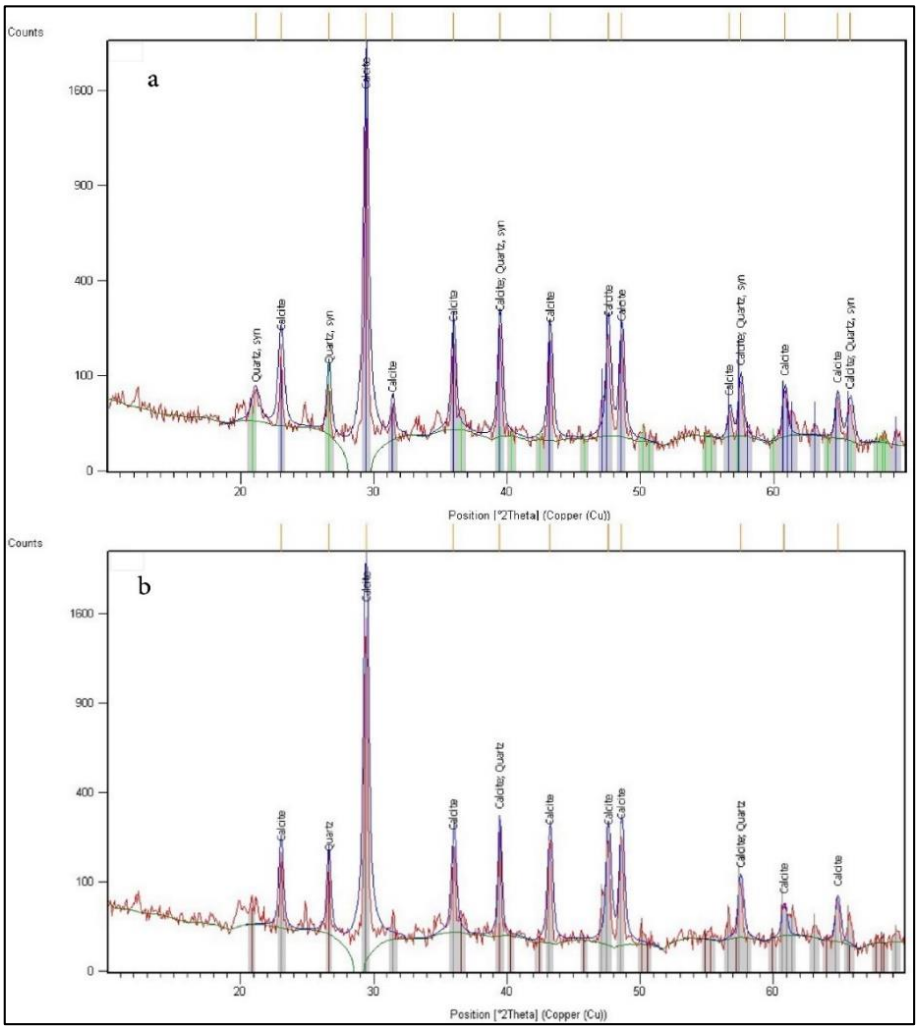


Figure 5: XRD charts of Sarmord Formation from the Qaiwan section.
**a)** Sample DLQ3, **b)** Sample DLQ2.

Table 1: Major oxide, trace elements, and REE concentrations of the brown detrital-limestone, Sarmord Formation.

| Major oxides | | | | | | | | | | | | | | | | | |
|---|---|---|---|---|---|---|---|---|---|---|---|---|---|---|---|---|---|
| Section | Sample | $SiO_2$ | $Al_2O_3$ | $Fe_2O_3$ | CaO | MgO | $Na_2O$ | $K_2O$ | $TiO_2$ | MnO | $P_2O_5$ | $Cr_2O_3$ | SrO | BaO | LOI | Total | |
| Qaiwan | DLQ1 | 12.80 | 5.33 | 6.24 | 38.90 | 0.77 | 0.04 | 0.40 | 0.28 | 0.12 | 0.09 | 0.006 | 0.04 | 0.01 | 34.40 | 99.42 | |
| | DLQ2 | 9.66 | 5.14 | 7.65 | 39.90 | 0.99 | 0.03 | 0.35 | 0.24 | 0.10 | 0.03 | 0.005 | 0.01 | 0.01 | 35.40 | 99.51 | |
| | DLQ3 | 13.20 | 6.60 | 7.13 | 36.40 | 0.78 | 0.04 | 0.59 | 0.31 | 0.19 | 0.06 | 0.006 | 0.03 | 0.01 | 33.20 | 98.55 | |
| | DLQ4 | 13.40 | 6.57 | 7.09 | 36.60 | 0.88 | 0.04 | 0.58 | 0.31 | 0.18 | 0.03 | 0.006 | 0.02 | 0.01 | 33.40 | 99.12 | |
| | DLQ5 | 12.90 | 6.51 | 7.24 | 35.00 | 2.87 | 0.05 | 0.62 | 0.31 | 0.18 | 0.13 | 0.006 | 0.04 | 0.01 | 33.90 | 99.76 | |
| | DLQ6 | 12.05 | 6.29 | 6.91 | 34.30 | 3.34 | 0.05 | 0.50 | 0.29 | 0.11 | 0.06 | 0.006 | 0.06 | 0.01 | 34.30 | 98.27 | |
| | DLQ7 | 13.20 | 6.48 | 7.28 | 33.80 | 3.68 | 0.05 | 0.52 | 0.32 | 0.14 | 0.06 | 0.005 | 0.06 | 0.01 | 33.90 | 99.51 | |
| | Average | 12.45 | 6.13 | 7.08 | 36.41 | 1.90 | 0.04 | 0.51 | 0.29 | 0.15 | 0.07 | 0.006 | 0.04 | 0.01 | 34.07 | 99.16 | |
| Barzinjah | DLB1 | 15.20 | 4.13 | 3.65 | 40.30 | 0.81 | 0.06 | 0.25 | 0.21 | 0.08 | 0.06 | 0.003 | 0.10 | 0.01 | 34.40 | 99.26 | |
| | DLB2 | 14.40 | 5.50 | 5.87 | 38.70 | 0.64 | 0.11 | 0.50 | 0.27 | 0.17 | 0.10 | 0.004 | 0.04 | 0.01 | 33.70 | 100.01 | |
| | DLB3 | 15.55 | 4.82 | 3.41 | 40.30 | 0.72 | 0.08 | 0.32 | 0.24 | 0.08 | 0.06 | 0.004 | 0.09 | 0.01 | 34.30 | 99.98 | |
| | DLB4 | 15.30 | 5.63 | 6.11 | 38.50 | 0.73 | 0.12 | 0.49 | 0.26 | 0.13 | 0.11 | 0.004 | 0.02 | 0.01 | 33.40 | 100.81 | |
| | DLB5 | 14.35 | 5.22 | 5.77 | 38.80 | 0.72 | 0.11 | 0.48 | 0.24 | 0.09 | 0.11 | 0.004 | 0.03 | 0.01 | 34.00 | 99.93 | |
| | DLB6 | 9.22 | 1.97 | 2.57 | 46.80 | 0.43 | 0.03 | 0.15 | 0.10 | 0.07 | 0.05 | 0.002 | 0.07 | 0.01 | 38.40 | 99.86 | |
| | Average | 14.00 | 4.55 | 4.56 | 40.57 | 0.68 | 0.09 | 0.37 | 0.22 | 0.10 | 0.08 | 0.004 | 0.06 | 0.01 | 34.70 | 99.98 | |
| Zewe | DLZ1 | 9.97 | 5.13 | 6.51 | 39.10 | 1.81 | 0.01 | 0.38 | 0.25 | 0.09 | 0.09 | 0.004 | 0.04 | 0.01 | 35.70 | 99.08 | |
| | DLZ2 | 11.25 | 5.62 | 5.87 | 37.70 | 2.64 | 0.01 | 0.40 | 0.28 | 0.09 | 0.09 | 0.004 | 0.05 | 0.01 | 35.50 | 99.50 | |
| | Average | 10.61 | 5.38 | 6.19 | 38.40 | 2.23 | 0.01 | 0.39 | 0.27 | 0.09 | 0.09 | 0.004 | 0.05 | 0.01 | 35.60 | 99.29 | |
| PAAS* | | 62.40 | 18.90 | 7.22 | 1.30 | 2.20 | 1.20 | 3.70 | 0.99 | 0.11 | 0.16 | … | … | ... | … | … | |

| Trace elements | | | | | | | | | | | | | | | | | | |
|---|---|---|---|---|---|---|---|---|---|---|---|---|---|---|---|---|---|---|
| Section | Sample | Ba | Sr | Cr | Zr | Hf | Nb | Rb | Th | U | V | Y | Co | Cu | Mo | Ni | Sc | Zn |
| Qaiwan | DLQ1 | 45.10 | 448.00 | 40.00 | 58.00 | 1.50 | 7.80 | 15.20 | 3.74 | 0.93 | 45.00 | 10.20 | 7.00 | 9.00 | 1.00 | 24.00 | 5.00 | 38.00 |
| | DLQ2 | 49.40 | 208.00 | 30.00 | 50.00 | 1.30 | 6.60 | 13.40 | 3.62 | 0.82 | 39.00 | 8.90 | 5.00 | 6.00 | 1.00 | 24.00 | 4.00 | 25.00 |
| | DLQ3 | 53.80 | 304.00 | 40.00 | 64.00 | 1.60 | 8.70 | 22.70 | 4.01 | 0.92 | 54.00 | 9.20 | 8.00 | 12.00 | 1.00 | 27.00 | 6.00 | 21.00 |
| | DLQ4 | 52.10 | 229.00 | 40.00 | 67.00 | 1.70 | 8.50 | 22.70 | 4.02 | 1.09 | 47.00 | 8.60 | 5.00 | 19.00 | 1.00 | 21.00 | 6.00 | 26.00 |
| | DLQ5 | 39.20 | 391.00 | 40.00 | 65.00 | 1.60 | 8.80 | 25.00 | 4.07 | 1.08 | 54.00 | 10.50 | 6.00 | 11.00 | 1.00 | 26.00 | 6.00 | 17.00 |
| | DLQ6 | 38.90 | 516.00 | 40.00 | 52.00 | 1.40 | 7.00 | 20.50 | 4.13 | 1.08 | 44.00 | 9.30 | 6.00 | 10.00 | 1.00 | 31.00 | 5.00 | 29.00 |
| | DLQ7 | 48.30 | 579.00 | 40.00 | 62.00 | 1.50 | 8.40 | 21.40 | 4.77 | 1.02 | 49.00 | 9.90 | 6.00 | 11.00 | 1.00 | 32.00 | 5.00 | 32.00 |
| | Average | 46.69 | 382.14 | 38.57 | 59.71 | 1.51 | 7.97 | 20.13 | 4.05 | 0.99 | 47.43 | 9.51 | 6.14 | 11.14 | 1.00 | 26.43 | 5.29 | 26.86 |
| Barzinjah | DLB1 | 54.10 | 827.00 | 20.00 | 47.00 | 1.30 | 5.90 | 10.10 | 3.19 | 1.35 | 34.00 | 11.90 | 4.00 | 6.00 | 1.00 | 23.00 | 3.00 | 57.00 |
| | DLB2 | 125.50 | 350.00 | 30.00 | 57.00 | 1.70 | 7.40 | 21.20 | 3.40 | 1.15 | 46.00 | 11.40 | 10.00 | 8.00 | 1.00 | 30.00 | 5.00 | 55.00 |
| | DLB3 | 47.40 | 700.00 | 20.00 | 49.00 | 1.30 | 6.30 | 12.40 | 3.17 | 1.09 | 36.00 | 9.70 | 4.00 | 6.00 | 1.00 | 26.00 | 4.00 | 50.00 |
| | DLB4 | 67.70 | 205.00 | 30.00 | 54.00 | 1.50 | 7.10 | 22.70 | 3.22 | 1.47 | 45.00 | 10.10 | 5.00 | 7.00 | 2.00 | 35.00 | 5.00 | 50.00 |
| | DLB5 | 124.00 | 263.00 | 30.00 | 50.00 | 1.30 | 6.70 | 22.20 | 2.86 | 1.56 | 54.00 | 10.10 | 4.00 | 7.00 | 2.00 | 23.00 | 4.00 | 43.00 |
| | DLB6 | 27.60 | 646.00 | 10.00 | 22.00 | 0.60 | 2.60 | 3.40 | 1.56 | 0.61 | 22.00 | 6.40 | 3.00 | 4.00 | 1.00 | 13.00 | 1.00 | 25.00 |
| | Average | 74.38 | 498.50 | 23.33 | 46.50 | 1.28 | 6.00 | 15.33 | 2.90 | 1.21 | 39.50 | 9.93 | 5.00 | 6.33 | 1.33 | 25.00 | 3.67 | 46.67 |
| Zewe | DLZ1 | 70.20 | 316.00 | 30.00 | 55.00 | 1.40 | 7.40 | 16.60 | 3.56 | 0.92 | 42.00 | 9.30 | 5.00 | 6.00 | 1.00 | 19.00 | 4.00 | 39.00 |
| | DLZ2 | 59.80 | 396.00 | 30.00 | 58.00 | 1.50 | 7.80 | 17.20 | 3.74 | 1.02 | 52.00 | 10.20 | 5.00 | 6.00 | 1.00 | 18.00 | 5.00 | 52.00 |
| | Average | 65.00 | 356.00 | 30.00 | 56.50 | 1.45 | 7.60 | 16.90 | 3.65 | 0.97 | 47.00 | 9.75 | 5.00 | 6.00 | 1.00 | 18.50 | 4.50 | 45.50 |
| PAAS* | | 650.00 | 200.00 | 110.00 | 210.00 | 5.00 | 19.00 | 160.00 | 14.60 | 3.10 | ##### | 27.00 | 23.00 | 50.00 | 1.50 | 55.00 | 16.00 | 85.00 |

| Rare Earth Elements (REE's) | | | | | | | | | | | | | | | | | | |
|---|---|---|---|---|---|---|---|---|---|---|---|---|---|---|---|---|---|---|
| Section | Sample | La | Ce | Pr | Nd | Sm | Eu | Gd | Tb | Dy | Ho | Er | Tm | Yb | Lu | LREE | HREE | REE |
| Qaiwan | DLQ1 | 13.90 | 29.20 | 3.47 | 13.50 | 2.78 | 0.61 | 2.51 | 0.34 | 1.92 | 0.35 | 0.95 | 0.14 | 0.88 | 0.12 | 63.46 | 7.21 | 70.67 |
| | DLQ2 | 13.50 | 27.30 | 3.17 | 11.80 | 2.29 | 0.45 | 1.94 | 0.28 | 1.73 | 0.32 | 0.88 | 0.12 | 0.74 | 0.12 | 58.51 | 6.13 | 64.64 |
| | DLQ3 | 14.30 | 28.30 | 3.22 | 12.20 | 2.08 | 0.43 | 1.97 | 0.28 | 1.75 | 0.34 | 1.01 | 0.15 | 0.90 | 0.14 | 60.53 | 6.54 | 67.07 |
| | DLQ4 | 13.80 | 27.70 | 3.08 | 11.40 | 2.13 | 0.45 | 1.79 | 0.27 | 1.62 | 0.31 | 0.85 | 0.13 | 0.82 | 0.12 | 58.56 | 5.91 | 64.47 |
| | DLQ5 | 14.90 | 31.40 | 3.59 | 13.80 | 2.94 | 0.60 | 2.49 | 0.37 | 2.07 | 0.39 | 1.05 | 0.16 | 0.93 | 0.13 | 67.23 | 7.59 | 74.82 |
| | DLQ6 | 13.90 | 28.60 | 3.17 | 12.10 | 2.33 | 0.51 | 1.96 | 0.29 | 1.71 | 0.34 | 0.99 | 0.15 | 0.88 | 0.14 | 60.61 | 6.46 | 67.07 |
| | DLQ7 | 15.70 | 32.70 | 3.68 | 13.80 | 2.63 | 0.52 | 2.29 | 0.32 | 1.91 | 0.37 | 1.02 | 0.14 | 0.92 | 0.14 | 69.03 | 7.11 | 76.14 |
| | Average | 14.29 | 29.31 | 3.34 | 12.66 | 2.45 | 0.51 | 2.14 | 0.31 | 1.82 | 0.35 | 0.96 | 0.14 | 0.87 | 0.13 | 62.56 | 6.71 | 69.27 |
| Barzinjah | DLB1 | 13.10 | 25.70 | 2.99 | 11.30 | 2.60 | 0.75 | 2.41 | 0.35 | 1.88 | 0.36 | 0.96 | 0.13 | 0.93 | 0.13 | 56.44 | 7.15 | 63.59 |
| | DLB2 | 13.80 | 29.50 | 3.29 | 12.30 | 2.91 | 0.58 | 2.64 | 0.37 | 1.91 | 0.36 | 1.07 | 0.13 | 0.95 | 0.12 | 62.38 | 7.55 | 69.93 |
| | DLB3 | 11.90 | 23.60 | 2.69 | 10.00 | 2.10 | 0.50 | 1.89 | 0.28 | 1.58 | 0.31 | 0.90 | 0.12 | 0.74 | 0.11 | 50.79 | 5.93 | 56.72 |
| | DLB4 | 12.60 | 25.50 | 2.89 | 10.90 | 2.52 | 0.51 | 2.19 | 0.31 | 1.73 | 0.33 | 1.09 | 0.15 | 0.95 | 0.11 | 54.92 | 6.86 | 61.78 |
| | DLB5 | 11.50 | 22.90 | 2.66 | 9.80 | 2.31 | 0.48 | 2.11 | 0.29 | 1.59 | 0.32 | 0.93 | 0.12 | 0.84 | 0.12 | 49.65 | 6.32 | 55.97 |
| | DLB6 | 6.60 | 12.70 | 1.50 | 5.20 | 1.14 | 0.30 | 1.07 | 0.15 | 0.89 | 0.18 | 0.56 | 0.07 | 0.50 | 0.05 | 27.44 | 3.47 | 30.91 |
| | Average | 11.58 | 23.32 | 2.67 | 9.92 | 2.26 | 0.52 | 2.05 | 0.29 | 1.60 | 0.31 | 0.92 | 0.12 | 0.82 | 0.11 | 50.27 | 6.21 | 56.48 |
| Zewe | DLZ1 | 13.60 | 28.20 | 3.19 | 11.70 | 2.36 | 0.51 | 2.03 | 0.31 | 1.67 | 0.32 | 0.91 | 0.13 | 0.74 | 0.12 | 59.56 | 6.23 | 65.79 |
| | DLZ2 | 14.70 | 29.70 | 3.32 | 12.30 | 2.38 | 0.51 | 2.09 | 0.33 | 1.79 | 0.34 | 0.99 | 0.14 | 0.85 | 0.14 | 62.91 | 6.67 | 69.58 |
| | Average | 14.15 | 28.95 | 3.26 | 12.00 | 2.37 | 0.51 | 2.06 | 0.32 | 1.73 | 0.33 | 0.95 | 0.14 | 0.80 | 0.13 | 61.24 | 6.45 | 67.69 |
| PAAS* | | 38.20 | 78.60 | 8.83 | 33.90 | 5.55 | 1.08 | 4.66 | 0.77 | 4.68 | 0.99 | 2.85 | 0.41 | 2.82 | 0.43 | ##### | 17.61 | 183.77 |

Table 2: Correlation coefficient of major and trace elements for brown detrital limestone of the Sarmord Formation.

| | SiO2 | Al2O3 | Fe2O3 | CaO | MgO | Na2O | K2O | TiO2 | MnO | P2O5 | Cr2O3 | SrO | LOI | Ba | Sr | Cr | Zr | Hf | Nb | Rb | Th | U | V | Y | Co | Cu | Mo | Ni | Sc | Zn | REE |
|---|---|---|---|---|---|---|---|---|---|---|---|---|---|---|---|---|---|---|---|---|---|---|---|---|---|---|---|---|---|---|---|
| SiO2 | 1.00 | | | | | | | | | | | | | | | | | | | | | | | | | | | | | | |
| Al2O3 | 0.30 | 1.00 | | | | | | | | | | | | | | | | | | | | | | | | | | | | | |
| Fe2O3 | -0.14 | 0.85 | 1.00 | | | | | | | | | | | | | | | | | | | | | | | | | | | | |
| CaO | -0.28 | -0.95 | -0.78 | 1.00 | | | | | | | | | | | | | | | | | | | | | | | | | | | |
| MgO | -0.21 | 0.49 | 0.46 | -0.69 | 1.00 | | | | | | | | | | | | | | | | | | | | | | | | | | |
| Na2O | 0.77 | 0.06 | -0.15 | -0.02 | -0.34 | 1.00 | | | | | | | | | | | | | | | | | | | | | | | | | |
| K2O | 0.32 | 0.93 | 0.79 | -0.86 | 0.37 | 0.21 | 1.00 | | | | | | | | | | | | | | | | | | | | | | | | |
| TiO2 | 0.32 | 0.98 | 0.81 | -0.94 | 0.51 | 0.01 | 0.88 | 1.00 | | | | | | | | | | | | | | | | | | | | | | | |
| MnO | 0.26 | 0.72 | 0.63 | -0.60 | 0.11 | 0.13 | 0.85 | 0.70 | 1.00 | | | | | | | | | | | | | | | | | | | | | | |
| P2O5 | 0.29 | 0.18 | 0.09 | -0.19 | 0.13 | 0.42 | 0.32 | 0.19 | 0.14 | 1.00 | | | | | | | | | | | | | | | | | | | | | |
| Cr2O3 | 0.07 | 0.85 | 0.81 | -0.78 | 0.37 | -0.16 | 0.78 | 0.84 | 0.68 | -0.02 | 1.00 | | | | | | | | | | | | | | | | | | | | |
| SrO | 0.22 | -0.46 | -0.74 | 0.26 | 0.11 | -0.04 | -0.56 | -0.39 | -0.50 | -0.14 | -0.47 | 1.00 | | | | | | | | | | | | | | | | | | | |
| LOI | -0.76 | -0.82 | -0.52 | 0.75 | -0.09 | -0.50 | -0.79 | -0.81 | -0.66 | -0.24 | -0.62 | 0.27 | 1.00 | | | | | | | | | | | | | | | | | | |
| Ba | 0.37 | 0.11 | 0.07 | -0.03 | -0.29 | 0.62 | 0.23 | 0.08 | 0.09 | 0.46 | -0.19 | -0.29 | -0.33 | 1.00 | | | | | | | | | | | | | | | | | |
| Sr | 0.16 | -0.48 | -0.70 | 0.27 | 0.11 | -0.10 | -0.58 | -0.40 | -0.46 | -0.22 | -0.42 | 0.98 | 0.31 | -0.39 | 1.00 | | | | | | | | | | | | | | | | |
| Cr | 0.10 | 0.92 | 0.90 | -0.89 | 0.49 | -0.09 | 0.87 | 0.92 | 0.71 | 0.15 | 0.93 | -0.53 | -0.68 | 0.00 | -0.49 | 1.00 | | | | | | | | | | | | | | | |
| Zr | 0.34 | 0.94 | 0.78 | -0.86 | 0.36 | -0.01 | 0.86 | 0.97 | 0.74 | 0.22 | 0.78 | -0.43 | -0.81 | 0.15 | -0.46 | 0.87 | 1.00 | | | | | | | | | | | | | | |
| Hf | 0.45 | 0.90 | 0.70 | -0.80 | 0.25 | 0.17 | 0.82 | 0.92 | 0.73 | 0.28 | 0.69 | -0.42 | -0.86 | 0.31 | -0.46 | 0.79 | 0.96 | 1.00 | | | | | | | | | | | | | |
| Nb | 0.29 | 0.95 | 0.81 | -0.88 | 0.42 | -0.03 | 0.87 | 0.98 | 0.72 | 0.27 | 0.80 | -0.45 | -0.78 | 0.14 | -0.47 | 0.89 | 0.99 | 0.94 | 1.00 | | | | | | | | | | | | |
| Rb | 0.39 | 0.91 | 0.77 | -0.84 | 0.37 | 0.33 | 0.97 | 0.86 | 0.75 | 0.44 | 0.68 | -0.56 | -0.81 | 0.37 | -0.61 | 0.82 | 0.84 | 0.83 | 0.85 | 1.00 | | | | | | | | | | | |
| Th | 0.15 | 0.91 | 0.80 | -0.93 | 0.66 | -0.19 | 0.73 | 0.94 | 0.57 | -0.01 | 0.80 | -0.24 | -0.66 | -0.11 | -0.22 | 0.88 | 0.88 | 0.80 | 0.89 | 0.68 | 1.00 | | | | | | | | | | |
| U | 0.78 | 0.28 | 0.02 | -0.29 | -0.09 | 0.76 | 0.31 | 0.24 | 0.04 | 0.48 | -0.05 | -0.02 | -0.63 | 0.59 | -0.12 | 0.10 | 0.26 | 0.37 | 0.24 | 0.48 | 0.07 | 1.00 | | | | | | | | | |
| V | 0.28 | 0.86 | 0.74 | -0.80 | 0.38 | 0.14 | 0.88 | 0.85 | 0.61 | 0.48 | 0.66 | -0.52 | -0.71 | 0.38 | -0.57 | 0.81 | 0.85 | 0.80 | 0.88 | 0.90 | 0.69 | 0.40 | 1.00 | | | | | | | | |
| Y | 0.66 | 0.38 | 0.13 | -0.42 | 0.12 | 0.43 | 0.28 | 0.44 | 0.17 | 0.51 | 0.10 | 0.16 | -0.62 | 0.46 | 0.10 | 0.24 | 0.48 | 0.61 | 0.47 | 0.38 | 0.38 | 0.66 | 0.44 | 1.00 | | | | | | | |
| Co | 0.18 | 0.54 | 0.50 | -0.47 | 0.08 | 0.17 | 0.58 | 0.58 | 0.71 | 0.24 | 0.50 | -0.32 | -0.51 | 0.35 | -0.30 | 0.57 | 0.56 | 0.67 | 0.57 | 0.53 | 0.49 | -0.04 | 0.49 | 0.40 | 1.00 | | | | | | |
| Cu | 0.22 | 0.71 | 0.57 | -0.63 | 0.19 | -0.07 | 0.75 | 0.69 | 0.78 | -0.21 | 0.75 | -0.36 | -0.60 | -0.12 | -0.32 | 0.73 | 0.70 | 0.63 | 0.66 | 0.63 | 0.62 | 0.05 | 0.50 | -0.03 | 0.33 | 1.00 | | | | | |
| Mo | 0.40 | 0.01 | 0.00 | 0.04 | -0.27 | 0.70 | 0.15 | -0.08 | -0.11 | 0.47 | -0.20 | -0.34 | -0.26 | 0.51 | -0.41 | -0.06 | -0.08 | -0.02 | -0.06 | 0.32 | -0.28 | 0.74 | 0.25 | 0.12 | -0.24 | -0.17 | 1.00 | | | | |
| Ni | 0.59 | 0.60 | 0.43 | -0.63 | 0.26 | 0.61 | 0.57 | 0.57 | 0.45 | 0.23 | 0.42 | -0.15 | -0.75 | 0.18 | -0.15 | 0.49 | 0.46 | 0.55 | 0.47 | 0.61 | 0.53 | 0.48 | 0.41 | 0.48 | 0.50 | 0.23 | 0.29 | 1.00 | | | |
| Sc | 0.33 | 0.96 | 0.79 | -0.87 | 0.35 | 0.08 | 0.92 | 0.96 | 0.80 | 0.25 | 0.85 | -0.50 | -0.82 | 0.11 | -0.52 | 0.90 | 0.96 | 0.93 | 0.96 | 0.89 | 0.83 | 0.24 | 0.86 | 0.39 | 0.61 | 0.72 | -0.01 | 0.55 | 1.00 | | |
| Zn | 0.51 | -0.22 | -0.45 | 0.21 | -0.26 | 0.46 | -0.33 | -0.16 | -0.41 | 0.28 | -0.53 | 0.37 | -0.11 | 0.52 | 0.25 | -0.40 | -0.11 | 0.08 | -0.14 | -0.16 | -0.23 | 0.55 | -0.11 | 0.61 | -0.02 | -0.47 | 0.28 | 0.12 | -0.19 | 1.00 | |
| REE | 0.25 | 0.85 | 0.74 | -0.86 | 0.54 | -0.05 | 0.68 | 0.90 | 0.54 | 0.27 | 0.69 | -0.25 | -0.69 | 0.11 | -0.25 | 0.80 | 0.89 | 0.88 | 0.90 | 0.69 | 0.92 | 0.22 | 0.73 | 0.67 | 0.60 | 0.43 | -0.19 | 0.55 | 0.82 | 0.03 | 1.00 |

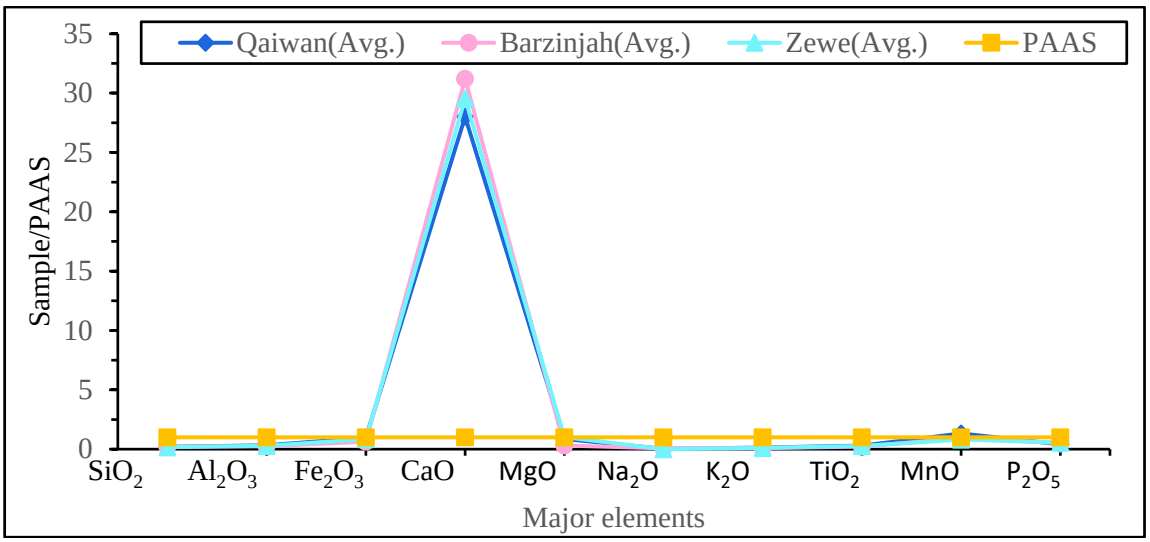


Figure 6: Post Archaean Australian Shale (PAAS) values of (Taylor & McLennan, 1985) normalized oxide patterns for the brown detrital limestone of the Sarmord Formation.

**4.2. Trace elements**

Trace element abundances in brown detrital bed limestones of Sarmord formation are given in (Table 1). The range and average of the trace element contents in the Qaiwan section show the following results:: Sr (208 to 579) ppm (avg. 382.14) ppm, Zr (50 to 67) ppm (average 59.71) ppm, Ba (38.9 to 53.8) ppm (average 46.69) ppm, V (39 to 54) ppm (average 47.43) ppm, Cr (30 to 40) ppm (average 38.57) ppm, Ni (21 to 32) ppm (average 26.43) ppm, Zn (17 to 38) ppm (average 26.86) ppm, Rb (13.4 to 25) ppm (average 20.13) ppm, Cu (6 to 19) ppm (average 11.14) ppm, Y (8.6 to 10.5) ppm (average 9.51) ppm, Nb (6.6 to 8.8) ppm (average 7.97) ppm, Co (5 to 8) ppm (average 6.14) ppm, Sc (4 to 6) ppm (average 5.29) ppm, and very low concentrations of Th, Hf, U, and Mo (< 5) ppm.

In the Barzinja section: Sr (205 to 827) ppm (average 498.5) ppm, Zr (22 to 57) ppm (average 46.5) ppm, Ba (27.6 to 125.5) ppm (average 74.38) ppm, V (22 to 54) ppm (average 39.5) ppm, Cr (10 to 30) ppm (average 23.33) ppm, Ni (13 to 35) ppm (average 25) ppm, Zn (25 to 57) ppm (average 46.67) ppm, Rb (3.4 to 22.7) ppm (average 15.33) ppm, Cu (4 to 8) ppm (average 6.33) ppm, Y (6.4 to 11.9) ppm (avg. 9.93) ppm, Nb (2.6 to7.4) ppm (average 6) ppm, Co (3 to 10) ppm (average 5) ppm, Sc (1 to 5) ppm (average 3.67) ppm, and very low concentration of Th, Hf, U and Mo (< 5) ppm.

In the Zewe section: Sr (316 to 394) ppm (average 356) ppm, Zr (55 to 58) ppm (average 56.5) ppm, Ba (59.8 to 70.2) ppm (average 65) ppm, V (42 to 52) ppm (average 47) ppm, Cr (30 to30) ppm (average 30) ppm, Ni (18 to 19) ppm (average 18.5) ppm, Zn (39 to 52) ppm (average 45.5) ppm, Rb (16.6 to 17.2) ppm (average16.9) ppm, Cu (6 to 6) ppm (average 6) ppm, Y (9.3 to 10.2) ppm (average 9.75) ppm, Nb (7.4 to7.8) ppm (average 7.6) ppm, Co (5 to 5) ppm (average 5) ppm, Sc (4 to 5) ppm (average 4.5) ppm, and very low concentration of Th, Hf, U and Mo (< 5) ppm. A spider diagram (Taylor & McLennan, 1985) depicts PAAS normalized trace element values. The average concentration of most trace elements is less than the average values of the PAAS except Sr, which has a greater concentration value. Generally, the brown detrital limestone samples of the Sarmord Formation compared to PAAS, it is significantly low in trace elements. except that of Sr, which is high and geochemically associated with calcite. Mo is near the PAAS value and a mild increase of Nb, U, and Zn is detected due to the detrital content in the studied limestones (Figure 7).

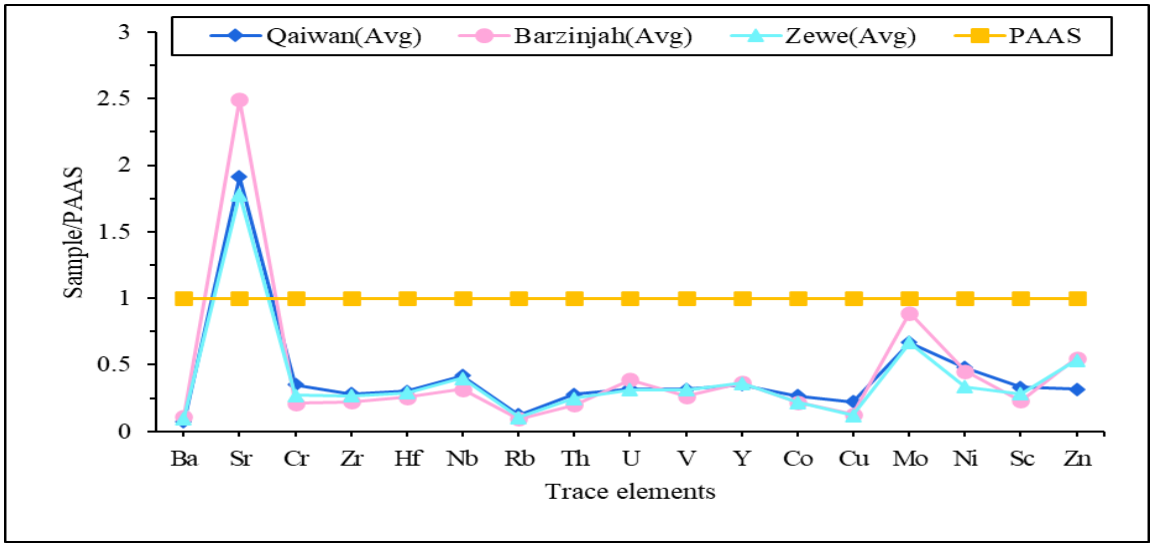


Figure 7: Post Archaean Australian Shale (PAAS) normalized trace element patterns for the Sarmord Formation's brown detrital limestone. The values of PAAS are from (Taylor & McLennan, 1985).

**4.3. Rare earth elements (REEs)**

The REEs concentration of the studied limestone samples is listed in (Table 1). The range and average of the trace element contents in the Qaiwan section are La (13.5 to 15.70) ppm (avg. 14.29) ppm, Ce (27.30 to 32.70) ppm (avg. 29.31) ppm, Pr (3.08 to 3.68) ppm (average 3.34) ppm, Nd (11.40 to 13.80) ppm (average 12.66) ppm, Sm (2.08 to 2.94) ppm (average 2.45) ppm, Gd (1.79 to 2.51) ppm (average 2.14) ppm, Dy (1.62 to 2.07) ppm (average 1.82) ppm and very low concentration of Eu, Tb, Ho, Er, Tm, Yb, and Lu (< 1) ppm. In the Barzinja section are La (6.60 to 13.80) ppm (average 11.58)ppm, Ce (12.70 to 29.50) ppm (average 23.32) ppm, Pr (1.50 to 3.29) ppm (average 2.67) ppm, Nd (5.20 to 12.30) ppm (average 9.92) ppm, Sm (1.14 to 2.91) ppm (average 2.26) ppm, Gd (1.07 to 2.64) ppm (average 2.05) ppm, Dy (0.89 to 1.91) ppm (average 1.60) ppm and very low concentration of Eu, Tb, Ho, Er, Tm, Yb, and Lu (< 1) ppm.

In the Zewe section are: La (13.60 to 14.70) ppm (average 14.15) ppm, Ce (28.20 to 29.70) ppm (average 28.95) ppm, Pr (3.19 to 3.32) ppm (average 3.26) ppm, Nd (11.70 to 12.30) ppm (average 12.00) ppm, Sm (2.36 to 2.38) ppm (avg. 2.37) ppm, Gd (2.03 to 2.09) ppm (avg. 2.06) ppm, Dy (1.67 to 1.79) ppm (average 1.73) ppm and very low concentration of Eu, Tb, Ho, Er, Tm, Yb and Lu (< 1) ppm.

The REEs average (ΣREE) is (69.27) ppm for Qaiwan brown detrital limestone, (56.48) ppm for Barzinjah brown detrital limestone and 67.69 ppm for Zewe brown detrital limestone, the ΣREE in all sections is less than the PAAS value (183.77) ppm (Table 1). The LREE concentration varies from (58.51 to 69.03) ppm, (27.44 to 62.38) ppm, and (59.56 to 62.91) ppm and HREE content varies from (5.91 to 7.59) ppm, (3.47 to 7.55) ppm and (6.23 to 6.67) ppm in Qaiwan, Barzinjah and Zewe sections, respectively (Table 1). The ΣREE shows a positive correlation with most major and trace elements except CaO and LOI (Table 2). A spider figure illustrates the PAAS normalized rare earth element quantities (Figure 8) (Taylor & McLennan, 1985).

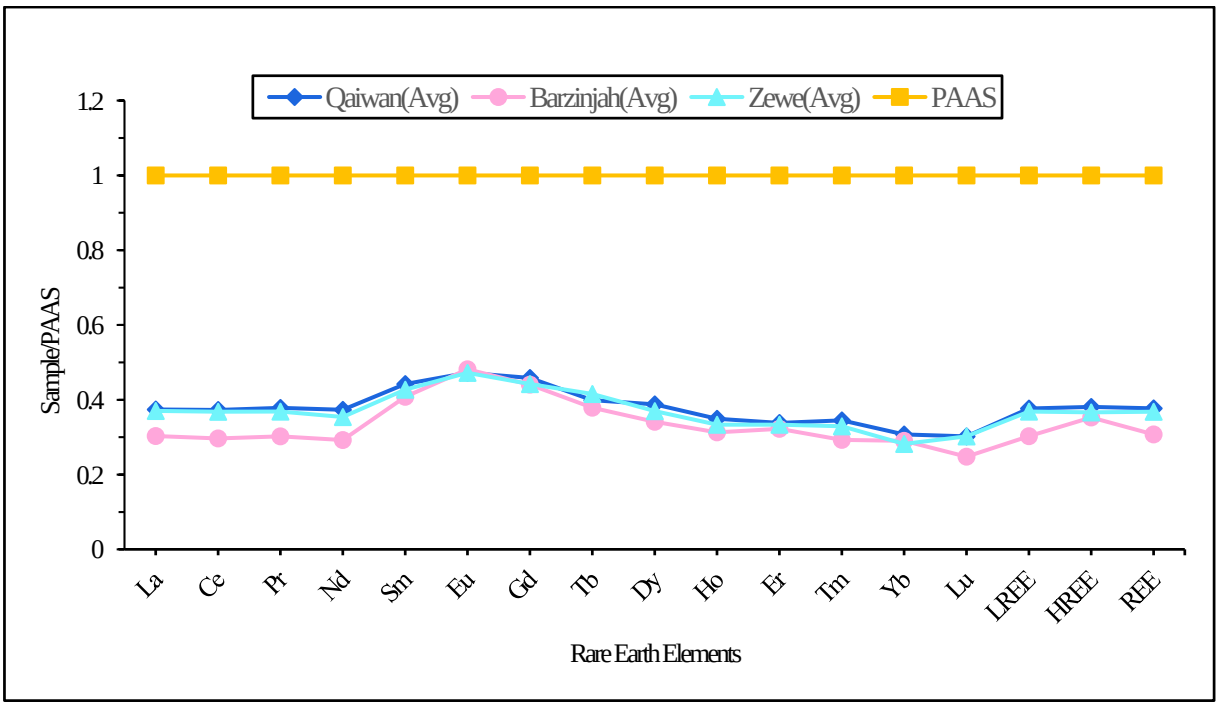


Figure 8: Post Archean Australian Shale (PAAS) normalized REEs patterns for the brown detrital limestone samples of the Sarmord Formation. PAAS values were taken from (Taylor & McLennan, 1985).

## 5. DISCUSSION

The mineralogy and element composition of these samples will be used to interpret the results of this investigation. Our samples show traces of clay and quartz grain of less than 2% as detected from the thin sections. The average CaO concentration in the limestone of all sections is near to each other, and the fluctuations in CaO content in all samples are very low, implying that these sections are chemically homogenous limestones. Because CaO is mostly formed from carbonates, it exhibits a considerable positive correlation with LOI over all sections (Table 2). CaO shows a strong negative relation with $Al_2O_3$, $TiO_2$, $K_2O$, $Fe_2O_3$, $Cr_2O_3$, MgO, and MnO demonstrating that carbonate phases dominate CaO control and explains the detrital content in the studied limestones which contain a small amount of amorphous iron oxide which is not detected by XRD. The low content of MgO in all studied samples is due to the deficiency of dolomite and/or dolomitization with dominant microcrystalline calcite is the only major carbonate mineral. The major impurities observed by XRD and petrography are silicates.

Regarding the open ocean environment the place where limestone is deposited, major elements ($Fe_2O_3$ and MnO, except for CaO) of these studied limestone successions show a large positive correlation with $Al_2O_3$ (Zhang et al., 2017). On the spider diagram, major oxides have been shown normalized using PAAS values (Figure 6) (Taylor & McLennan, 1985). The figure shows that the samples with the greatest CaO concentrations are more stable and have fewer impurities. which are confirmed by XRD analysis and thin sections. (Figures 4 and 5). Generally, the brown detrital limestone samples of the Sarmord Formation are Compared to PAAS, the samples have a significant trace element depletion. except that of Sr which is geochemically associated with calcite (Brookins & Watson, 1969). Mo is near the PAAS value due to the detrital content in the studied limestones (Voegelin et al., 2010)

(Figure 7). The PAAS plot REE normalized concentrations also show notable depletion due to the source area weathering and transportation through marine water (Figure 8).

Negative correlations between ΣREEs and CaO and strong positive correlations between ΣREEs and elements such as Co, Al, Ni, Rb, Si, Cu, Ti, Nb, and V imply that the small amount of detrital substances mostly regulated the observed changes in REE concentrations in the limestone. According to geochemical data, plagioclase and diagenetic processes may be responsible for the distinct positive Eu anomalies in the brown detrital limestone layers and may be considered as syn-hydrothermal fluids incorporated with sea water (Danielson et al., 1992) (Table 2).

### 5.1. Provenance

The use of the geochemical composition of sedimentary rocks has an important role in understanding the nature of source rocks (McLennan et al., 1993); (Roser & Korsch, 1988). When the source rocks weather, the majority of elements, particularly Na, Mg, K, and Ca, partly leak away. However, Ti, Zr, and Al can be regarded as basically immobile elements because the oxides and hydroxides of these elements have low solubility in low-temperature aqueous solutions (Morgan & Stumm, 1981); (Wesolowski, 1992). Sediments are derived from felsic rocks if the $Al_2O_3/TiO_2$ ratio ranges from 21 to 80, sediments are derived from intermediate rocks if the ratio of $Al_2O_3/TiO_2$ ranges from 8 to 21, and if the ratio of $Al_2O_3/TiO_2$ ranges from 3 to 8, that means the sediments are derived from basic rocks (Hayashi et al., 1997). The $Al_2O_3/TiO_2$ ratio of brown detrital limestone of Sarmord Formation samples in the Qaiwan, Barzinjah and Zewe sections (Table 3) varies from 19.03 to 21.68 (avg. 20.83), 19.66 to 21.75 (avg. 20.53) and 20.07 to 20.52 (avg. 20.29) respectively, which indicates the mixed source rocks and/or felsic as a whole. Grigsby (1992) suggested a discrimination diagram to identify the provenance source for sedimentary clastic facies as a provenance indicator (Figure 9a). On the plot of $TiO_2 + V_2O_3$ vs MgO/ (MgO + $Al_2O_3$) the samples display felsic plutonic source rocks.

Table 3. Paleoredox parameters, paleoclimate parameters, and paleosalinity parameters for studied samples of Sarmord Formation.

| Section | Sample no. | Paleoredox | | | Paleoclimate | | Paleosalanity | | Provenance |
|---|---|---|---|---|---|---|---|---|---|
| | | U/Th | V/Cr | Ni/Co | Sr/Cu | C-value | Rb/K | Sr/Ba | $Al_2O_3/TiO_2$ |
| Qaiwan | DLQ1 | 0.24 | 1.12 | 3.42 | 49.77 | 0.15 | 0.0045 | 9.93 | 19.04 |
| | DLQ2 | 0.22 | 1.30 | 4.80 | 34.66 | 0.18 | 0.0046 | 4.21 | 21.42 |
| | DLQ3 | 0.22 | 1.35 | 3.38 | 25.33 | 0.19 | 0.0046 | 5.65 | 21.29 |
| | DLQ4 | 0.27 | 1.17 | 4.20 | 12.05 | 0.18 | 0.0047 | 4.39 | 21.19 |
| | DLQ5 | 0.26 | 1.35 | 4.33 | 35.54 | 0.19 | 0.0048 | 9.97 | 21.00 |
| | DLQ6 | 0.26 | 1.10 | 5.16 | 51.60 | 0.18 | 0.0049 | 13.26 | 21.69 |
| | DLQ7 | 0.21 | 1.22 | 5.33 | 52.63 | 0.19 | 0.0049 | 11.98 | 20.25 |
| | Average | 0.24 | 1.23 | 4.37 | 37.37 | 0.18 | 0.0047 | 8.48 | 20.84 |
| Barzinjah | DLB1 | 0.42 | 1.70 | 5.75 | 137.83 | 0.08 | 0.0048 | 15.28 | 19.67 |
| | DLB2 | 0.33 | 1.53 | 3.00 | 43.75 | 0.14 | 0.0051 | 2.78 | 20.37 |
| | DLB3 | 0.34 | 1.80 | 6.50 | 116.66 | 0.08 | 0.0046 | 14.76 | 20.08 |
| | DLB4 | 0.45 | 1.50 | 7.00 | 29.28 | 0.15 | 0.0055 | 3.02 | 21.65 |
| | DLB5 | 0.54 | 1.80 | 5.75 | 37.57 | 0.14 | 0.0055 | 2.12 | 21.75 |
| | DLB6 | 0.39 | 2.20 | 4.33 | 161.50 | 0.05 | 0.0027 | 23.40 | 19.70 |
| | Average | 0.41 | 1.70 | 5.38 | 87.76 | 0.11 | 0.0047 | 10.23 | 20.54 |
| Zewe | DLZ1 | 0.25 | 1.40 | 3.80 | 52.66 | 0.15 | 0.0052 | 4.50 | 20.52 |
| | DLZ2 | 0.27 | 1.73 | 3.60 | 66.00 | 0.14 | 0.0051 | 6.62 | 20.07 |
| | Average | 0.26 | 1.56 | 3.70 | 59.33 | 0.15 | 0.0052 | 5.56 | 20.30 |

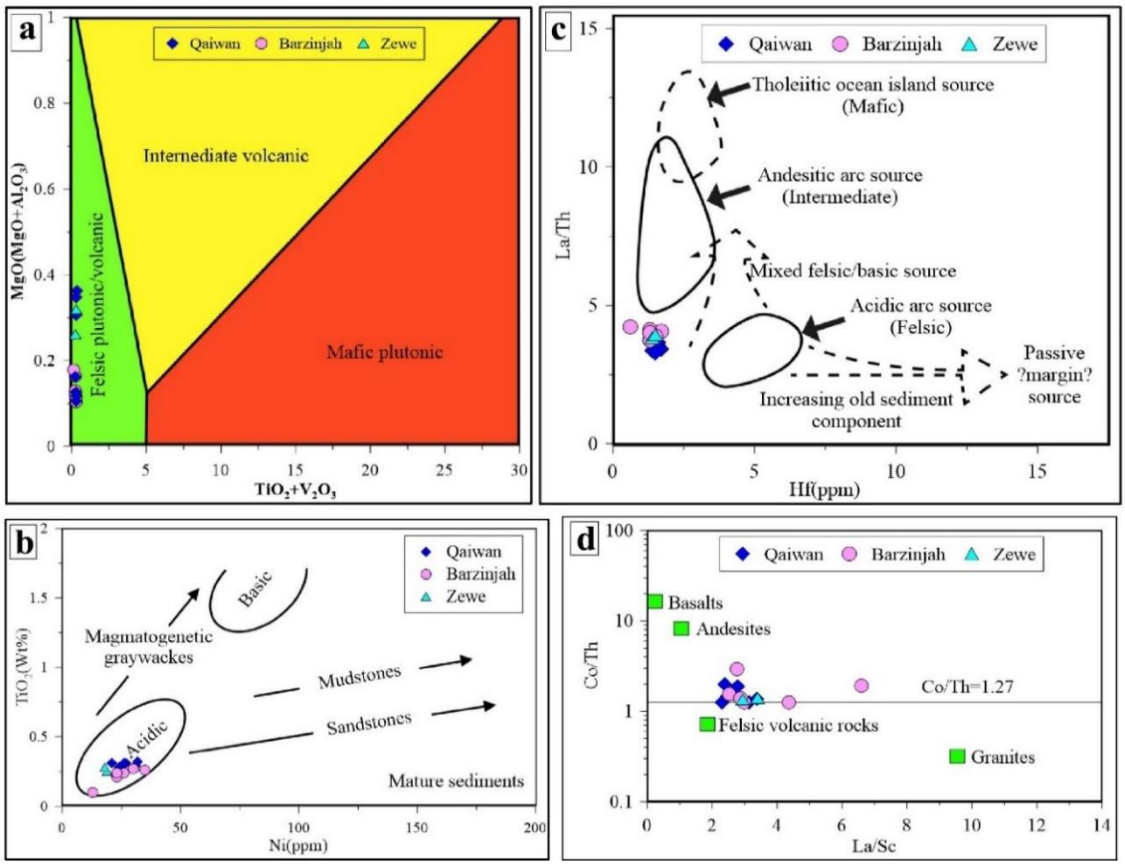


Figure 9: **a)** Discrimination plot of $TiO_2+V_2O_3$ vs $MgO/(MgO+Al_2O_3)$ for studied samples (diagram after Grigsby, 1992); **b)** $TiO_2$ vs Ni bivariate diagram for the studied samples from Sarmord Formation (after Floyd et al., 1989); **c)** La/Th vs Hf bivariate diagram for brown detrital limestone of Sarmord Formation (after Floyd & Leveridge, 1987) and **d)** La/Sc vs Co/Th diagram for studied samples (Gu et al., 2002).

Immobile trace elements such as $TiO_2$, Ni, and Zr are geochemical proxies to discriminate the provenance of the sediments (Hayashi et al., 1997); (Floyd et al., 1989). In the provenance discrimination ($TiO_2$ vs Ni) diagram of Hayashi et al. (1997), the samples of the Sarmord Formation from all sections plotted in the field of acidic(felsic) rocks (Figure 9b). A plot of La/Th versus Hf shows useful bulk rock discrimination between different sources and arc compositions (Floyd & Leveridge, 1987). On a Hf versus La/Th bivariate (Figure 9c) samples of Sarmord Formation are scattered between fields of felsic and andesitic suggesting the mixed felsic/ intermediate source rocks for the brown detrital limestone of Sarmord Formation. REE, Cr, Co, Th, and Sc are useful elements due to their brief residency in the water column and rapid incorporation into the record of sedimentary, monitoring the compositions of source areas Taylor & McLennan (1985). Co/Th and La/Sc ratios are reliable indications of the compositions of source rocks (Gu et al., 2002) because mafic rocks are depleted in Th and La and enriched in Co and Sc compared to felsic rocks (Cullers, 1994). On the plot of Co/Th versus La/Sc (Figure 9d) (Gu et al., 2002), the data reflect felsic-intermediate source rocks. There are considerable differences between the ratios of La/Sc, La/Co, and Th. /Sc, Cr/Th, and Th/Cr in felsic and mafic rocks, which might place limitations on the provenance composition (Cox et al., 1995). Comparing the ratios of the brown beds of Sarmord Formation in all sections with sediments sourced from felsic and mafic rocks of UCC and PAAS values of Taylor & McLennan (1985) as well as Cullers (1994). These ratios,

according to the comparison, fall into the range of felsic rocks (Table 4). These felsic rocks are possibly the main outcrops of an area during the Early Cretaceous that coincides with the present Western Desert, in this connection many carbonate formations are mentioned by Bellen et al. (1959) and Sissakian & Mohammed (2007) during Jurassic and Early Cretaceous. These brown beds are possibly affected too by remote volcanic arcs that were surrounding Neotethys during the Early Cretaceous from which some REE and trace elements are transported from volcanic arcs shown in Figure (10). This effect is reflected by the anomalous location in the diagram of Hf - La/TH (Figure 9c).

Table 4: Ratios of elements for the brown detrital limestone of Sarmord Formation in comparison with fine fractions source rocks derived from felsic and mafic.

| Elemental ratios | Range of sediments | | UCC[2] | PAAS[2] | Average of studied sections | | |
|---|---|---|---|---|---|---|---|
| | Felsic Rocks | Mafic Rocks | | | Qaiwan | Barzinjah | Zewe |
| La/Sc | 2.50 – 16.30 | 0.43 – 0.86 | 2.21 | 2.4 | 2.74 | 3.68 | 3.17 |
| La/Co | 1.80 – 13.80 | 0.14 – 0.38 | 1.76 | 1.66 | 2.37 | 2.53 | 2.83 |
| Th/Sc | 0.84 – 20.50 | 0.05 – 0.22 | 0.79 | 0.9 | 0.77 | 0.90 | 0.81 |
| Cr/Th | 4.00 – 15.00 | 25.00 – 500 | 7.76 | 7.53 | 9.54 | 7.93 | 8.22 |
| Th/Cr | 0.13 – 2.70 | 0.018 – 0.046 | 0.13 | 0.13 | 0.10 | 0.13 | 0.12 |

**1)** (Cullers, 1994)**; 2)** (Taylor & McLennan, 1985)**; 3) This study.**

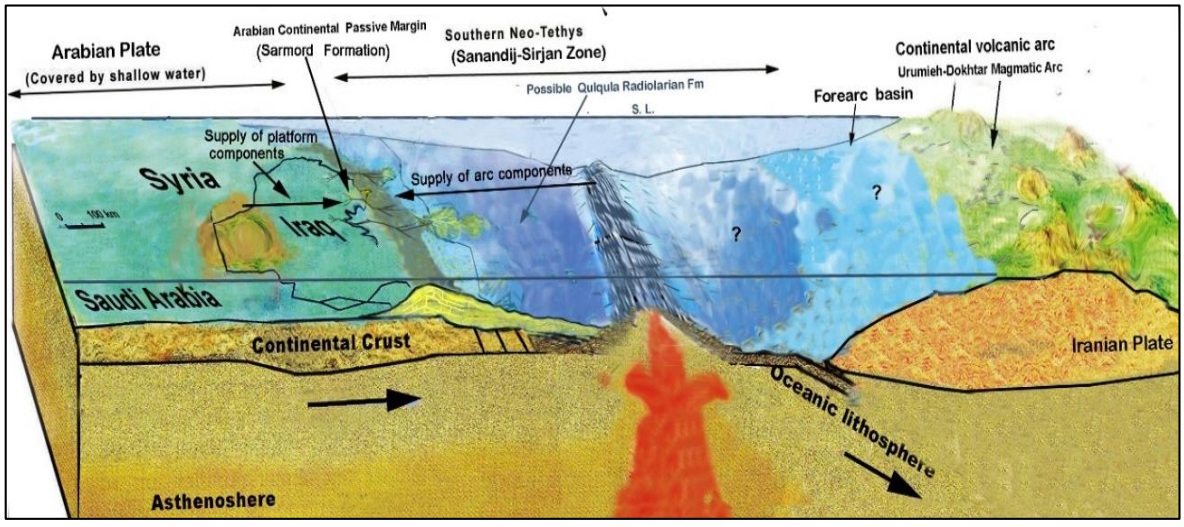


Figure 10: Location of Sarmord Formation on the Arabian platform which is geochemically affected weakly by island arc, deep marine water in addition to the geochemistry of its original location of the platform (modified from Mirza et al., 2021).

### 5.2. Tectonic setting and depositional model

Limestone forms in a variety of tectonic settings, including continental margin, oceanic margin, oceanic floor, and inland (Wilson, 1975). Primarily, during these varieties of depositional environments trace elements and REE are introduced which are mainly influenced by the basin plate tectonic environment (Murray et al., 1991). Zhang et al. (2017) plot a triangular diagram for the Sr – Rb – Ba and Mirza et al. (2021) plot a diagram for the Sr/Ba versus Sr/Rb, the studied samples of brown detrital limestone reveal that these samples are distributed between the continental margin and inland field (Figure 11a and b). This is due

to the low Ba and Sr concentration in differentiation with open ocean limestones (Zhang et al., 2017). Older marine carbonates and weathering of volcanic ash layers are two plausible origins of the increased Sr in the shale (Cochran et al., 2010). This is evident by drawing a tectonic model based on the previous model constructed by Mirza et al. (2021), which explained and showed that the SSZ of the southern part of Neo-Tethys was a deep basin during the Early Cretaceous, so these detrital limestones are transported from the erosion of the platform into deep marine and interbedded with the green marl and weakly supplied by some elements from the arc components (Figure 10). They are well-sorted lithoclast due to transportation for very long distances by turbidity current.

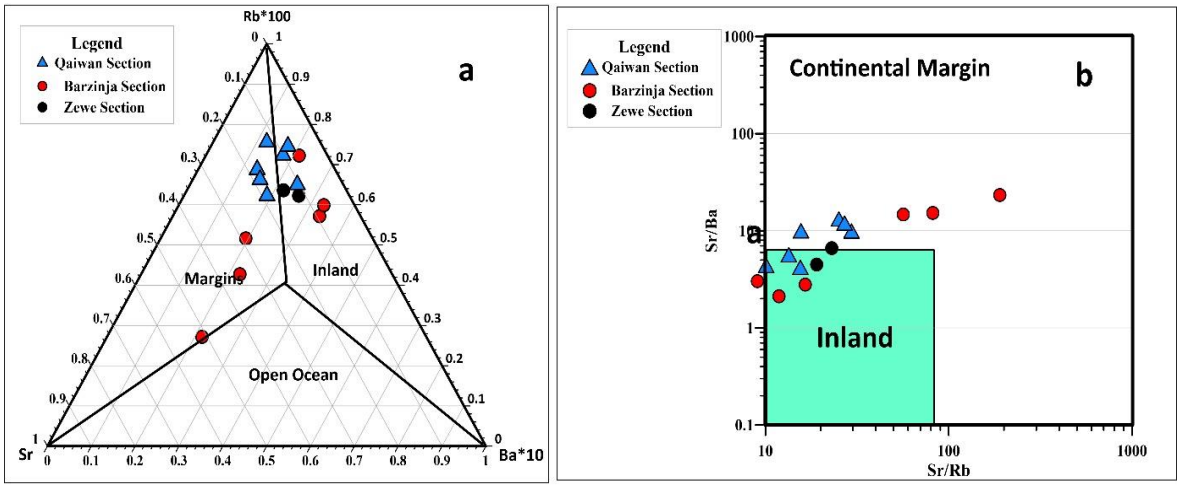


Figure 11: **a**) Rb - Sr - Ba ternary diagram (after Zhang et al., 2017); **b**) Scatter plot between Sr/Ba and Sr/Rb indicating a continental Inland margin depositional environment for brown detrital limestone samples. (after Mirza et al., 2021).

### 5.3. Paleoredox

Tyson & Pearson (1991) used the words oxic, dysoxic, suboxic, and anoxic to describe the oxygenation of bottom water (Table 5). When hydrogen sulfide is present in the water column, anoxic conditions are also known as euxinic circumstances (Tribovillard et al., 2006). Euxinic environments are those in which the water column contains free $H_2S$ Trace element ratios are useful for assessing sedimentary bottom water conditions because the behavior of specific elements associated with organic and/or terrigenous components is influenced by redox conditions (Hallberg, 1976) The following ratios U/Th, V/Cr, and Ni/Co are employed in this study to identify the paleoredox state since (Jones & Manning, 1994) considered them to be the most accurate indicators.

A redox indicator may be made from the ratio of uranium to thorium (Adams & Weaver, 1958). According to Jones & Manning (1994) U/Th below 0.75 indicates oxic circumstances, whereas those between 0.75 and 1.25 indicate dysoxic conditions, and those beyond 1.25 indicate suboxic and anoxic conditions.. In the present study, the U/Th value is less than 0.75 in all sections (Figure 12 and Table 3) which indicates oxic conditions.

Numerous research has proposed and used the ratio V/Cr as an indicator of paleoredox (e.g., Ernst, 1970). Values of V/Cr ratios less than 2 indicate oxic circumstances, between 2 to 4.25 imply dysoxic situations, and it indicates suboxic and anoxic conditions when it is more than 4.25 (Jones & Manning, 1994). The V/Cr value is less than 2 in all sections except one

sample in the Barzinjah section is 2.2 (Figure 12 and Table 3), this indicates oxic conditions in both Qaiwan and Zewe sections while oxic to dysoxic in the Barzinjah section.

Table 5: Terminology for the description of bottom water oxygenation (Tyson & Pearson, 1991).

| Term | Oxygen Concentration (ml $I^{-1}$) |
|---|---|
| Oxic | 2.0 – 8.0 |
| Dysoxic | 0.2 – 2.0 |
| Suboxic | 0.0 – 0.2 |
| Anoxic | 0.0 ($H_2S$) |

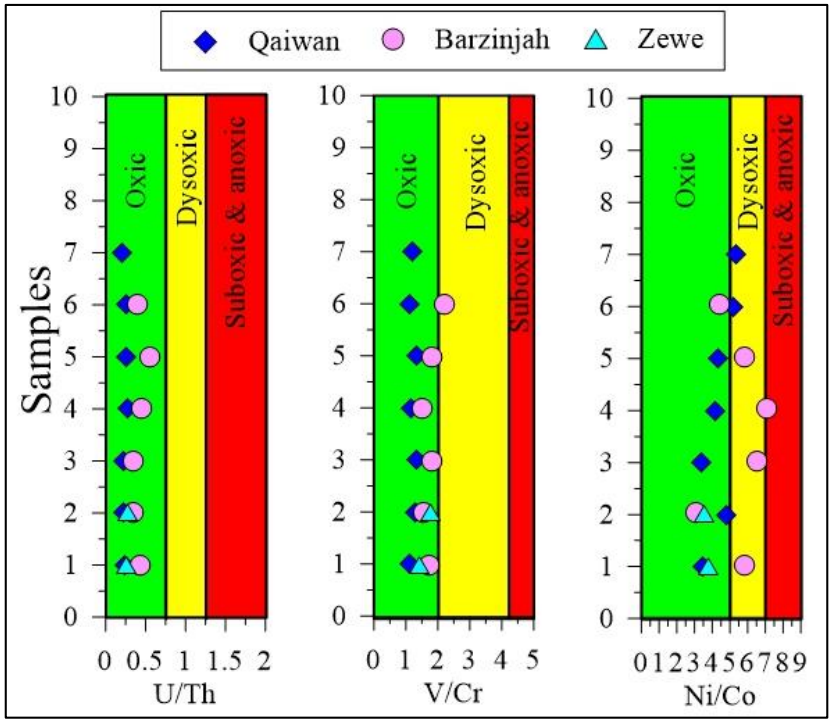


Figure 12: The distribution of U/Th, V/Cr, and Ni/Co ratios in the study area (fields after Jones & Manning, 1994).

Ni/Co has also been utilized as a redox index (e.g., Dypvik, 1984). Ni/Co ratios of less than five imply an oxic environment, those of five to seven dysoxic, and those of seven or more suboxic and anoxic (Jones & Manning, 1994). Ni/Co ratio in Qaiwan section range from 3.37 to 5.33 (avg. 4.37), in Barzinjah section range from 3 to 7 (avg. 5.38) and in Zewe section range from 3.6 to 3.8 (avg. 3.7), which indicates oxic to dysoxic conditions in Qaiwan and Barzinjah sections while oxic conditions in Zewe section (Figure 12 and Table 3). The samples from the Qaiwan Barzinjah and Zewe sections have very low average Sr/Ca ratios (0.0014, 0.0017, and 0.0013, respectively) compared to the deep-sea carbonate samples (0.00525) reported by Turekian (1964) indicating a shallow marine environment for the Sarmord Formation.

Deep marine shale is distinguished from shallow marine and freshwater shale in (Figure 13), which displays V against $Al_2O_3$ (after Mortazavi et al., 2014). Consistently, the examined samples were found in a shallow sea environment. This paleoenvironmental interpretation is correlated with the above paleo-redox conditions (oxic to dysoxic conditions). So the origin of

the detrital brown beds was continental or shallow marine but deposited in deep marine and associated (during deposition) with ammonite and nano fossil.

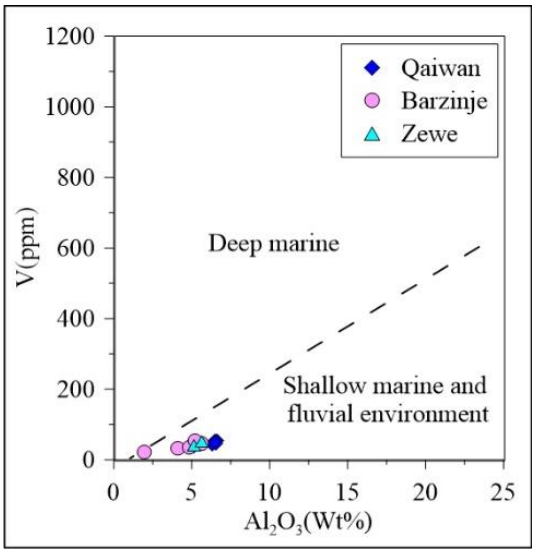


Figure 13: Plots of $Al_2O_3$ vs V for the brown detrital limestone of Sarmord Formation for paleoenvironmental reconstruction (after Mortazavi et al., 2014).

**5.4. Paleoclimate**

The geochemistry and mineralogy of sediments are significantly impacted by climate (Yan et al., 2010). The best chemical maturity trend as a function of climate can be shown in the $SiO_2$ versus total ($Al_2O_3$ + $K_2O$ + $Na_2O$) diagram (Suttner & Dutta, 1986). Based on the binary diagram of $SiO_2$ versus ($Al_2O_3$ + $K_2O$ + $Na_2O$), the samples of the Sarmord Formation indicated deposition in an arid climatic condition in all studied sections (Figure 14a).

To determine the paleoenvironmental conditions of fine-grained siliciclastic rocks, the concentrations of some major oxides and trace elements were used (Roy & Roser, 2013). Rogers & Adams (1969) proposed the ratio of Σ (Fe + Mn + Cr + Ni + V + Co)/ Σ (Ca + Mg + Sr + Ba + K + Na) (termed as C-value) as a climate proxy. In the present study, the C-values of the Sarmord Formation samples range from 0.15 to 0.19% (avg. of 0.18% in the Qaiwan section, 0.05 to 0.15% (avg. of 0.11% in the Barzinjah section and 0.14 to 0.15% (avg. of 0.15% in the Zewe section (Table 3), reflecting a generally arid climatic condition for the source area (present western desert) (Figure 14b).

Additionally, the Sr/Cu ratio has been used for palaeoclimatic investigations (e.g., Meng et al., 2012). Sr in the sediment being produced leaches away, and the Sr/Cu ratio in the deposited sediment is decreased when the environment is more humid and warmer to encourage greater weathering (Deng & Qian, 1993). According to Lerman (1978), Sr/Cu ratios between 1.3 to 5.0 indicate a warm humid climate, whereas ratios over 5.0 indicate a hot, arid climate. The samples from the s hot arid conditions. Rb/K and Sr/Ba ratios suggest brackish water conditions for the brown detrital limestone beds of the Sarmord Formation.

**5.5. Paleosalanity**

The paleosalinity of brown detrital limestone of the Sarmord Formation was measured by using the Rb/K ratio and Sr/Ba ratio (Table 3). Degens et al. (1957) proposed Rb as a possible indicator of paleoenvironment stating that Rb is concentrated in marine shales. (Campbell & Williams, 1965) suggested that the elemental ratio of Rb/K less than 0.004 suggests freshwater conditions, 0.004 to 0.006 suggests a brackish water condition, and more than 0.006 designates a fully marine water environment. The Rb/K ratio of brown detrital limestone in the Sarmord Formation ranges from 0.0045 to 0.0049% (avg. 0.0047%) in the

Qaiwan section, 0.0027 to 0.0055% (avg. 0.0047%) in Barzinjah section, and 0.0051 to 0.0052% (avg. 0.0052) in Zewe section, indicating a brackish water sedimentary environment in all sections (Table 3).

The geochemical behavior of strontium (Sr) and barium (Ba) in various sedimentary environments is different (Liu et al., 1984; The elemental ratio of Sr/Ba is often accepted as an empirical indicator of paleosalinity (B. J. Liu, 1980). A Sr/Ba ratio of 0.2 distinguishes between fresh water and brackish sediments, whereas a ratio of 0.5 distinguishes between brackish and marine sediments (Wei & Algeo, 2020). The Sr/Ba ratio ranges from 4.21 to 13.26 (avg. 8.48), 2.12 to 23.4 (10.23), and 4.50 to 6.62 (5.56) in the Qaiwan, Barzinjah, and Zewe sections respectively, which indicate marine water condition in all studied sections (Table 3).

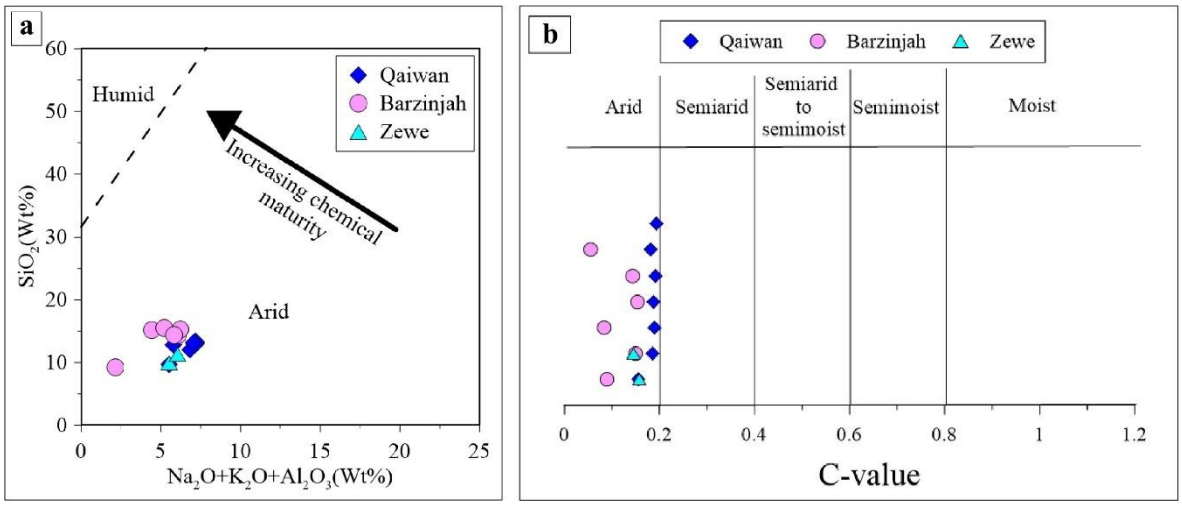


Figure 14: **a**) binary $SiO_2$ vs ($Na_2O + K_2O + Al_2O_3$) diagram indicating paleoclimatic condition for the studied samples (after Suttner & Dutta, 1986) and (**b**) the C-value [Σ (Fe + Mn + Cr + Ni + V + Co)/ Σ (Ca + Mg + Sr + Ba + K + Na)] for the studied samples of Sarmord Formation, reflecting palaeoclimate (after Rogers & Adams, 1969).

## 6. CONCLUSION

The brown detrital limestone beds of the Sarmord Formation in the Qaiwan, Barzinjah, and Zewe sections are similar to each other geochemically and show enrichment in CaO concentration (It has a diluting influence on the other major oxides, trace elements, and REE's) in addition to the enrichment in Sr content with dedolomitization during the depositional environment. The absence of dolomitization indicates high-energy facies to open a high-oxygen marine environment. The concentration of REE explains the high fugacity of the depositional environment. The relation between Rb – Sr – Ba elements using scatter and triangular diagrams explains a continental margin and island arc tectonic settings for the source rock. The ratios of ($Al_2O_3/TiO_2$, La/Sc, La/Co, Th/Sc, Cr/Th and Th/Cr), and the diagrams ($TiO_2 + V_2O_3$ Vs MgO/ ($MgO + Al_2O_3$), $TiO_2$ Vs Ni, La/Th Vs Hf and La/Sc Vs Co/Th) reveal that the brown detrital limestone beds of Sarmord Formation were sourced from felsic and intermediate rocks. The Mosul High and western desert were the terrains of granite exposure and carbonate deposition which performed as a source area for the limestone -beds. All of the samples are distributed between the continental margin and inland field with low Ba and higher Rb concentrations. Tectonically these brown detrital limestones belong to Early Cretaceous platform erosion and were transported to deep marine and interbedded with

the green marl far away from the weak effect of siliciclastic volcanic activity which forms the formation as a whole. The V/Cr, U/Th, Ni/Co, and Sr/Ca ratios as well as the $Al_2O_3$ Vs V diagram imply a shallow marine oxic to the dysoxic environment. The paleoclimate indicators including C-value [ΣFe + Mn + Cr + Ni + V + Co)/ Σ (Ca + Mg + Sr + Ba + K + Na)], Sr/Cu ratio, and $SiO_2$ versus ($Al_2O_3$ + $K_2O$ + $Na_2O$) diagram refer the hot arid conditions. Rb/K and Sr/Ba ratios suggest brackish water conditions for the brown detrital limestone beds of the Sarmord Formation.

## ACKNOWLEDGMENTS

The authors would like to thank Professor Dr. Kamal H. Karim for his help in the identification of thin sections throughout the fieldwork. We also want to thank the University of Sulaimani, Department of Geology for allowing us to use their laboratories, and also we would like to thank the ALS international laboratory in Canada for their accurate and precise (ICP-AES) and (ICP-MS) chemical analysis.

## REFERENCES

Adams, J. A. S., & Weaver, C. E. (1958). Thorium-to-uranium ratios as indicators of sedimentary processes: example of concept of geochemical facies. *AAPG Bulletin*, *42*(2), 387–430.

Ahmed, S. H., Qadir, B. O., & Müller, C. (2015). Age determinations of Cretaceous sequences based on calcareous nannofossils in Zagros Thrust and Folded Zone in Kurdistan Region-Iraq. *Journal of Zankoy Sulaimani*, 13–17.

Al-Samarraie, B. A. (2012). Petrograhpic study of the Sarmord Formation In North Zakho Area, Nw Iraq. *Iraqi Bulletin of Geology and Mining*, *8*(2), 45–63.

Bellen, R. C. Van, Dunnington, H. V., Wetzel, R., & Morton, D. (1959). Lexique Stratigraphic International. *Asie, Iraq*, *3*(10a), 333.

Bhatia, M. R., & Crook, K. A. W. (1986). Trace element characteristics of graywackes and tectonic setting discrimination of sedimentary basins. *Contributions to Mineralogy and Petrology*, *92*(2), 181–193.

Bjørlykke, K. (1974). Geochemical and mineralogical influence of Ordovician Island Arcs on epicontinental clastic sedimentation. A study of Lower Palaeozoic sedimentation in the Oslo Region, Norway. *Sedimentology*, *21*(2), 251–272.

Brookins, D. G., & Watson, K. D. (1969). The strontium geochemistry of calcite associated with kimberlite at Bachelor Lake, Quebec. *The Journal of Geology*, *77*(3), 367–371.

Buday, T. and Jassim, S. Z. (1984). *Tectonic Map of Iraq, Scale 1:1,000,000*. GEOSURV, Baghdad.

Buday, T. (1980). *The regional geology of Iraq: tectonism, magmatism and metamorphism* (Vol. 2). State Organization for Minerals, Directorate General for Geological Survey.

Campbell, F. A., & Williams, G. D. (1965). Chemical Composition of Shales of Mannville Group (Lower Cretaceous) of Central Alberta, Canada1. *AAPG Bulletin*, *49*(1), 81–87. https://doi.org/10.1306/A66334EA-16C0-11D7-8645000102C1865D

Chatton, M., & Hart, E. (1960). *Revision of the Tithonian to Albian Stratigraphy of Iraq*.

Cochran, J. K., Kallenberg, K., Landman, N. H., Harries, P. J., Weinreb, D., Turekian, K. K., Beck, A. J., & Cobban, W. A. (2010). Effect of diagenesis on the Sr, O, and C isotope composition of late Cretaceous mollusks from the Western Interior Seaway of North America. *American Journal of Science*, *310*(2), 69–88.

Cox, R., Lowe, D. R., & Cullers, R. L. (1995). The influence of sediment recycling and basement composition on evolution of mudrock chemistry in the southwestern United States. *Geochimica et Cosmochimica Acta*, *59*(14), 2919–2940.

Cullers, R. L. (1994). The controls on the major and trace element variation of shales, siltstones, and sandstones of Pennsylvanian-Permian age from uplifted continental blocks in Colorado to platform sediment in Kansas, USA. *Geochimica et Cosmochimica Acta*, *58*(22), 4955–4972.

Danielson, A., Möller, P., & Dulski, P. (1992). The europium anomalies in banded iron formations and the thermal history of the oceanic crust. *Chemical Geology*, *97*(1–2), 89–100.

Degens, E. T., Williams, E. G., & Keith, M. L. (1957). Environmental Studies of Carboniferous Sediments Part I: Geochemical Criteria for Differentiating Marine from Fresh-Water Shales1. *AAPG Bulletin*, *41*(11), 2427–2455. https://doi.org/10.1306/0BDA59A5-16BD-11D7-8645000102C1865D

Deng, H. ., & Qian, K. (1993). *Sedimentary Geochemistry and Environment Analysis*. Gansu Science & Technology Press.

Dypvik, H. (1984). Geochemical compositions and depositional conditions of Upper Jurassic and Lower Cretaceous Yorkshire clays, England. *Geological Magazine*, *121*(5), 489–504. https://doi.org/DOI: 10.1017/S0016756800030028

Ernst, T. W. (1970). *Geochemical Facies Analysis*. Elsevier.

Fatah, S. S., Sarraj, R. H., Al-Qayim, B., Mohialdeen, I. M. J., Al-Jubouri, Q. M., Khanaqa, P. A. A., & Mohammed, Z. K. (2023). Sedimentology, Palynofacies, and Hydrocarbon Potential of the Early Cretaceous Sarmord Formation from Khabbaz and Kirkuk Oil Fields, Northern Iraq. *The Iraqi Geological Journal*, 110–137.

Floyd, P. A., & Leveridge, B. E. (1987). Tectonic environment of the Devonian Gramscatho basin, south Cornwall: framework mode and geochemical evidence from turbiditic sandstones. *Journal of the Geological Society*, *144*(4), 531–542.

Floyd, P. A., Winchester, J. A., & Park, R. G. (1989). Geochemistry and tectonic setting of Lewisian clastic metasediments from the Early Proterozoic Loch Maree Group of Gairloch, NW Scotland. *Precambrian Research*, *45*(1–3), 203–214.

Grigsby, J. D. (1992). Chemical fingerprinting in detrital ilmenite; a viable alternative in provenance research? *Journal of Sedimentary Research*, *62*(2), 331–337.

Gu, X. X., Liu, J. M., Zheng, M. H., Tang, J. X., & Qi, L. (2002). Provenance and tectonic setting of the Proterozoic turbidites in Hunan, South China: geochemical evidence. *Journal of Sedimentary Research*, *72*(3), 393–407.

Hallberg, R. O. (1976). A geochemical method for investigation of palaeoredox conditions in sediments. *Ambio Special Report*, *4*(4), 139–147.

Hayashi, K.-I., Fujisawa, H., Holland, H. D., & Ohmoto, H. (1997). Geochemistry of∼ 1.9 Ga sedimentary rocks from northeastern Labrador, Canada. *Geochimica et Cosmochimica Acta*, *61*(19), 4115–4137.

Jassim, S. Z., & Goff, J. C. (2006). *Geology of Iraq*. DOLIN, sro, distributed by Geological Society of London.

Jones, B., & Manning, D. A. C. (1994). Comparison of geochemical indices used for the interpretation of palaeoredox conditions in ancient mudstones. *Chemical Geology*, *111*(1–4), 111–129.

Karim, K. H., Al-Dulaimy, S. I., Ahmad, P. M., & Al-Badrani, O. (2021). Stratigraphy and Nannofossil Biozonation of Sarmord Formation on the Qaywan Anticline in Sulaymaniyah Governorate, Northern Iraq. *The Iraqi Geological Journal*, 75–86.

Lerman, A. (1978). *Lakes Chemistry and Geology Physics*. Springer.

Liu, B. J. (1980). *Sedimentary Petrology. Geological Press*.

Liu, Y. J. ., Cao, L. M. ., Li, Z. L. ., Wang, H. N. ., Chu, T. Q. ., & Zhang, J. R. (1984). *Element Geochemistry*. Science Press.

McLennan, S. M., Hemming, S., McDaniel, D. K., & Hanson, G. N. (1993). *Geochemical approaches to sedimentation, provenance, and tectonics*.

Meng, Q., Liu, Z., Bruch, A. A., Liu, R., & Hu, F. (2012). Palaeoclimatic evolution during Eocene and its influence on oil shale mineralisation, Fushun basin, China. *Journal of Asian Earth Sciences*, *45*, 95–105. https://doi.org/hzttps://doi.org/10.1016/j.jseaes.2011.09.021

Mirza, T. A., Karim, K. H., Ridha, S. M., & Fatah, C. M. (2021). Major, trace, rare earth element, and stable isotope analyses of the Triassic carbonates along the northeastern Arabian Plate margin: a key to understanding paleotectonics and paleoenvironment of the Avroman (Biston) limestone formation from Kurdistan reg. *Carbonates and Evaporites*, *36*(4), 66.

Morgan, J. J., & Stumm, W. (1981). *Aquatic Chemistry-An Introduction Emphasizing Chemical Equilibria in Natural Waters*. New York, NY, John Wiley & Sons.

Mortazavi, M., Moussavi-Harami, R., Mahboubi, A., & Nadjafi, M. (2014). Geochemistry of the Late Jurassic–Early Cretaceous shales (Shurijeh Formation) in the intracontinental Kopet-Dagh Basin, northeastern Iran: implication for provenance, source weathering, and paleoenvironments. *Arabian Journal of Geosciences*, *7*, 5353–5366.

Murray, R. W., Ten Brink, M. R. B., Gerlach, D. C., Russ III, G. P., & Jones, D. L. (1991). Rare earth, major, and trace elements in chert from the Franciscan Complex and Monterey Group, California: assessing REE sources to fine-grained marine sediments. *Geochimica et Cosmochimica Acta*, *55*(7), 1875–1895.

Nesbitt, Hw., & Young, G. M. (1982). Early Proterozoic climates and plate motions inferred from major element chemistry of lutites. *Nature*, *299*(5885), 715–717.

Rogers, J. J. W. ., & Adams, J. A. S. (1969). Abundances in rock forming minerals (I), uranium minerals (II). In K. H. Wedepohl (Ed.), *The Handbook of Geochemistry* (pp. 92-D). Springer.

Roser, B. P., & Korsch, R. J. (1988). Provenance signatures of sandstone-mudstone suites determined using discriminant function analysis of major-element data. *Chemical Geology*, *67*(1–2), 119–139.

Roy, D. K., & Roser, B. P. (2013). Climatic control on the composition of Carboniferous–Permian Gondwana sediments, Khalaspir basin, Bangladesh. *Gondwana Research*, *23*(3), 1163–1171.

https://doi.org/https://doi.org/10.1016/j.gr.2012.07.006
Sissakian, V. K., & Mohammed, B. S. (2007). Stratigraphy. *Iraqi Bulletin of Geology and Mining*, *1*, 51–124.
Suttner, L. J., & Dutta, P. K. (1986). Alluvial sandstone composition and paleoclimate; I, Framework mineralogy. *Journal of Sedimentary Research*, *56*(3), 329–345.
Taylor, S. R., & McLennan, S. M. (1985). *The continental crust: its composition and evolution*.
Tribovillard, N., Algeo, T. J., Lyons, T., & Riboulleau, A. (2006). Trace metals as paleoredox and paleoproductivity proxies: an update. *Chemical Geology*, *232*(1–2), 12–32.
Turekian, K. K. (1964). SECTION OF GEOLOGICAL SCIENCES: THE GEOCHEMISTRY OF THE ATLANTIC OCEAN BASIN. *Transactions of the New York Academy of Sciences*, *26*(3 Series II), 312–330.
Tyson, R. V., & Pearson, T. H. (1991). Modern and Ancient Continental Shelf Anoxia, Geol. *Soc. Spec. Publ*, *58*.
Voegelin, A. R., Nägler, T. F., Beukes, N. J., & Lacassie, J. P. (2010). Molybdenum isotopes in late Archean carbonate rocks: implications for early Earth oxygenation. *Precambrian Research*, *182*(1–2), 70–82.
Wei, W., & Algeo, T. J. (2020). Elemental proxies for paleosalinity analysis of ancient shales and mudrocks. *Geochimica et Cosmochimica Acta*, *287*, 341–366. https://doi.org/https://doi.org/10.1016/j.gca.2019.06.034
Wesolowski, D. J. (1992). Aluminum speciation and equilibria in aqueous solution: I. The solubility of gibbsite in the system Na-K-Cl-OH-Al (OH) 4 from 0 to 100 C. *Geochimica et Cosmochimica Acta*, *56*(3), 1065–1091.
Wilson, J. L. (1975). Carbonate facies in geologic history Springer-Verlag. *New York*, *471*.
Yan, D., Chen, D., Wang, Q., & Wang, J. (2010). Large-scale climatic fluctuations in the latest Ordovician on the Yangtze block, south China. *Geology*, *38*(7), 599–602.
Zhang, K.-J., Li, Q.-H., Yan, L.-L., Zeng, L., Lu, L., Zhang, Y.-X., Hui, J., Jin, X., & Tang, X.-C. (2017). Geochemistry of limestones deposited in various plate tectonic settings. *Earth-Science Reviews*, *167*, 27–46.

## About the authors

**Dr. Sardar M. Ridha** is a lecturer at the University of Sulaimaniyah, College of Sciences, Dept. Geology. He is a member of the Kurdistan Geological Society and the Union of Iraqi Geologists. He got an M.Sc. In hydrogeochemistry/ University of Baghdad and Ph.D. in sedimentary geochemistry/University of Sulaimani. He is at present supervising one MSc student in the field of geochemistry. He has 12 years of experience in the oil field as a wellsite geologist starting from SOC in Basrah (North Rumaila, West Qurma, and Zubir oilfields for 7 years) and also as a senior wellsite geologist with (DNO, GasPlus, and DanaGas companies) in (Tawki, Benenan, Shewashan and Kormore fields) for 4 years separately.

**e-mail**: sardar.ridha@univsul.edu.iq

**Mr. Sehad A. Eminki** is an M.Sc. student at the University of Sulaimani, College of Sciences, Department of Geology. He graduated with a B.Sc. degree in 2018/2019 at the University of Duhok, College of Spatial Planning and Applied Geosciences, Department of Applied Geosciences.

**e-mail**: sehad.muhamed@univsul.edu.iq